THE UNIVERSITY OF CALGARY

Quantification of Interstitial Lipid *In Vivo* Using a Magnetic Resonance Image-Segmentation Technique

by

Richard James Schaan

A THESIS

SUBMITTED TO THE FACULTY OF GRADUATE STUDIES

IN PARTIAL FULFILMENT OF THE REQUIREMENTS FOR THE

DEGREE OF MASTER OF SCIENCE

FACULTY OF KINESIOLOGY

CALGARY, ALBERTA

APRIL, 1999

Abstract

The goal of the project was to (1) quantify interstitial lipid (IL) at selected sites in vivo, (2) compare intrasubject IL, and (3) compare IL with total body fat (TBF). Subjects consisted of twenty, male Caucasians ranging in TBF from 5-36%. Three MR slices (1.5 T, TR 500 ms, TE 17 ms) were taken from each right-sided limb segment (12 total slices). Image reconstruction was performed on computer program Viewdiff© with pixel intensity and region-of-interest analysis performed on Adobe Photoshop©. Adipose tissue volume was determined and converted to a percent lipid mass (of regional skeletal muscle mass). Densitometry was used to determine TBF. There was no intrasegmental variability for upper arm (UA) or thigh (UL) ($p>0.05$). The proximal forearm (FA) and medial calf (LL) slice were different ($p<0.05$) from the other two FA and LL slices, respectively. Mean(SE) %IL values were: UA 3.61 (0.19), FA 6.01 (0.44), UL 4.31 (0.39), and LL 4.11 (0.65). Overall mean percent interstitial lipid was 4.51% (0.33). Limb segments (%IL) were statistically different ($p<0.05$) from one another. Correlation of limb segment %IL was significant ($p<0.05$) with TBF for FA ($r=0.65$), UL ($r=0.63$), LL ($r=0.85$). UA ($r=0.37$) was not significantly correlated. ($p=0.1$). Correlation of mean %IL with TBF was significant ($r=0.87$; $p<0.01$). These data suggest (1) intersegmental variability (2) positive correlation between IL and TBF.

Acknowledgements

I would like to thank the following people for their assistance in the completion of this thesis.

My Lord and Savior, Jesus Christ for His great mercy and love.

Dr. Preston Wiley for his faith, understanding, confidence, and patience. The opportunities and advice that he has given me have contributed to my overall education as a researcher and as a human being.

Dr. Michael Hawes for igniting my love for anatomy and giving me great opportunities in my academic career.

Pierre Laforge for doing his job with enthusiasm, humility, and humanitarianism.

Dr. Adrian Crawley for answering a "billion" questions on MR analysis.

My committee members: Dr. Carla Wallace, Dr. Rita Aggarwala, and Dr. Barbara Olson.

Olympic Oval fund for financial support.

Human Performance Laboratory technicians Rosie Neil and Heather Philpot, and my volunteer assistant Jody Nicholson for their time, ingenuity, and effort.

My wife, Charlotte, for her love, support, and patience while I worked on this research. Thank you for always believing in me.

Dedication

To my Parents,

My mom,
for her unconditional love
and unnatural patience.

The loving memory of my father,
a man who sacrificed everything
to give me his time and love,
so that I may become a better man.

I love you both.

kyrie eleison

Table of Contents

List of Tables

List of Figures

Epigraph

Science is not the study of truth. Science is the study of hypotheses. If you want truth, go into Philosophy.

- Dr. Brian Lloyd, my Organic Chemistry professor, friend, and mentor, on the first day of class. This statement has shaped how I view Science and has given me a better appreciation of both it, and reality.

CHAPTER 1

INTRODUCTION

At the turn of the twentieth century, research in body composition was performed primarily on cadavers to assess various body components *in vitro*. *In vivo* tissue assessments were limited because of a lack of technology and a limited knowledge on body composition and tissue distribution. The vast majority of the research in the field of body composition has focussed primarily on the distribution and quantity of adipose tissue. In recent years, this research has been propagated by convincing epidemiological evidence linking obesity to health-related disorders and by a decrease in sport performance with obesity.

Early in the twentieth century, methods to quantify adipose tissue within the body *in vivo* were developed (Matiegka, 1921). Behnke (1942) developed densitometry (or hydrostatic weighing), an *in vivo* method capable of estimating total body lipid. Densitometry was a significant development in body composition research because it provided a potential reference upon which other techniques could be based. At present, there are several methods, such as anthropometric equations and bioelectric impedance, which are regressed against hydrostatic weighing (Martin *et. al.*, 1991). These methods offer various ways to estimate total body lipid *in vivo* but are incapable of investigating individual depots of adipose tissue within the body.

The field of body composition views adipose tissue as being compartmentalized within four sites in the human body (Wang *et. al.*, 1992):

1) Subcutaneous – directly underlying the skin.

2) Visceral - surrounding the thoracic and abdominal organs.

3) Bone Marrow - within the bone marrow cavity.

4) Interstitial – "residual lipid" in connective tissue, skin, interspersed within organs and also underlying the fascial sheaths within the muscle compartments.

The first two sites have been extensively studied using various *in vitro* and *in vivo* techniques primarily because of their extensiveness within the body as well as being more accessible when compared to the latter two compartments.

Until recently, research on interstitial lipid has been hampered by a lack of technology, permitting limited *in vitro* studies. Unfortunately, cadaveric studies on interstitial lipid are difficult because they tend to be time consuming, have a small number of representative samples, and must be drawn from very small cadaveric populations which tend to be elderly. Our knowledge of interstitial lipid is based on few cadaver studies (Mitchell *et. al.* 1945; Widdowson 1951; Forbes *et. al.*, 1953, Forbes *et. al.*, 1956; Moore *et. al.*, 1968). *In vivo* studies were limited because biochemical analysis of muscle biopsies was not feasible due to the large number of samples required to attain any statistical significance and other technologies were not able to perform

valid and accurate studies. With recent advances in the field of magnetic resonance imaging (MRI) and its subdiscipline chemical-shift imaging (CSI), valid, larger-scale research on interstitial lipid can be performed. This research may be of benefit to several disciplines.

The sport community may benefit from knowledge of interstitial lipid because its role during exercise is unknown. It is speculated that an individual may utilize interstitial lipid preferentially during exercise instead of mobilizing fat depots more distant from the energy-requiring muscles but no scientific evidence is available to support this.

The medical community and the general public are concerned with high adiposity because it is associated with various health-related disorders, such as cardiovascular disease and *diabetes mellitus* but little is known of interstitial lipid's contribution to overall adiposity.

1.1 Magnetic Resonance Imaging

Magnetic resonance imaging is ideal for *in vivo* investigation of lipid for several reasons. Unlike Computer Tomography (CT), the subjects are not exposed to any ionizing radiation. The data is collected relatively quickly and the generated image has a high resolution which enables the researcher to discriminate between different tissues. This technology has been utilized for the past twenty-five years with no known side-effects.

In biological samples the proton NMR spectrum is dominated by two peaks arising from water and aliphatic (CH_2) protons (Buxton *et. al.* 1986). Though many molecular structures contain CH_2 residues, the vast majority are associated with lipids (Brateman, 1986). Because of the difference in resonance frequency between water and lipids, MR images are capable of high-lighting the lipids within the scanned area. A region-of-interest (ROI) can then be defined to focus on the lipid within a specific area, such as the fascial compartment. With these qualities, MRI is an excellent method to quantify interstitial lipid *in vivo.*

1.2 Interstitial lipid - Definition

To understand which components are actually being quantified, the term "interstitial lipid" should be correctly defined. The term "interstitial" is derived from the Latin word *interstitium*: *inter* , meaning "between", *stit* referring to "space" and *-ium*, meaning "structure or tissue". The American Medical Association Encyclopedia of Medicine defines interstitial as "pertaining to or situated between parts or in the interspaces of a tissue" (Clayman, 1989).

Based on the previous categorization of adipose tissue or lipid belonging to one of four compartments, the interstitial compartment may be considered as the residual adipose tissue within the skin, connective tissue, muscle, organs, or residual areas. Because the layer of skin is typically less

than 2 mm in thickness (Martin *et. al.*, 1985), it is not readily identified on MR images. For the purpose of this study, our definition considered only the muscle and residual adipose and lipid within the fascial compartment and surrounding the vessels and nerves. MR images of transverse slices through extremity muscle compartments offer excellent views to image and quantify interstitial lipid. The generalizability of the extremity muscle compartments should be valid since over 75% of muscle mass is located in the limbs (Snyder *et. al.*, 1984), and is substantiated by anthropometric assessments of muscle mass using extremities for their assessments (Mateigka, 1921; McEvoy *et. al.*, 1982; Chumlea *et. al.*, 1986; Martin *et. al.*, 1990; Baumgartner *et. al.*, 1992).

The terms "lipid" and "fat" are often used interchangeably, though they refer to different molecular structures. Therefore, for the purpose of this study, both terms require definitions. In the field of body composition, researchers typically quantify or analyze lipids, not fat. Lipids are water insoluble organic compounds with a non-polar nature found in biological systems which can be extracted from tissues using organic solvents (Fessenden *et. al.*, 1990; Horton *et. al.*, 1993). Though all lipids share this common physical property, the abundance of lipids in biological systems is due to the variety of functions that they perform, including energy storage, thermal insulation and protection, and the formation of biological membranes. These functions are fulfilled by many classes of lipids, including phospholipids, triglycerides, prostaglandins, terpenes, and steroids.

Phospholipids are very abundant in biological systems because they are the major contributor to cell membranes (Fessenden *et. al.*, 1990; Stryer, 1975). Phospholipids are amphipathic molecules because they possess a hydrophilic dipolar-ion group and two long hydrophobic tails. This structural characteristic makes them excellent emulsifying agents and prevents the passage of water, ions, or polar molecules through a lipid bilayer membrane. Phospholipids also provide electrical insulation for nerve cells due to the presence of sphingolipids in the myelin sheath (Fessenden *et. al.*, 1990; Stryer, 1975).

The terms "fat" and "oil" refer specifically to triglycerides (Fessenden *et. al.*, 1990), hence "fats" are actually a subgroup of lipids. Triglycerides are the most abundant lipid (Fessenden *et. al.*, 1990) and are a major contributor to biological membranes, energy storage and thermal insulation. Triglycerides, or triacylglycerols, are comprised of a glycerol backbone esterified to three fatty acids, which are generally long, unbranched hydrocarbon chains. The fatty acid portions of triglyceride molecules are variable in their composition (Table 1.1), producing a variety of different triglycerides. Saturated fatty acids have no double bonds within the carbon chain and are most commonly associated with fats from animals and are usually present in a solid state at room temperature. Unsaturated or polyunsaturated fatty acids, typically associated with plants or vegetable oils, have at least one double bond present.

Table 1.1: Different types of fatty acids and their molecular compositions

Name of Acid	Structure
Saturated:	
Butyric	$CH_3(CH_2)_2CO_2H$
Palmitic	$CH_3(CH_2)_{14}CO_2H$
Stearic	$CH_3(CH_2)_{16}CO_2H$
Unsaturated:	
Palmitoleic	$CH_3(CH_2)_5CH=CH(CH_2)_7CO_2H$
Oleic	$CH_3(CH_2)_7CH=CH(CH_2)_7CO_2H$
Linoleic	$CH_3(CH_2)_4CH=CHCH_2CH=CH(CH_2)_7CO_2H$
Linolenic	$CH_3CH_2CH=CHCH_2CH=CHCH_2CH=CH(CH_2)_7CO_2H$
Arachidonic	$CH_3(CH_2)_4(CH=CHCH_2)_4(CH_2)_2CO_2H$

Prostaglandins are unique lipids that were originally found to be synthesized in the prostate gland but are now known to be synthesized in the lungs, liver, uterus and other organs (Fessenden *et. al.*, 1990). Though a prostaglandin's activity varies from one type of tissue to another, all types of prostaglandins are hormone-like compounds which alter the activity of the producing and adjoining cells. Prostaglandins are 20-carbon carboxylic acids with cyclopentane rings that are biosynthesized from 20-carbon unsaturated fatty acids (Appendix A).

Steroids are common biological compounds which have a structural conformation of four cyclic rings (Appendix A). Many steroids act as hormones and synthetic steroids have a variety of pharmaceutical applications, including the treatment of allergies and inflammation. The

most abundant steroid is cholesterol, which is found in most animal biological tissues and is an important structural component of cell membranes. Cholesterol is a precursor of androgens, estrogens, progestins, and cortisone, which are important and common steroids (Fessenden *et. al.*, 1990).

Due to the universal use of these terms, "total body fat" and "body fat" will be used throughout this research, instead of the correct form "total body lipid". Otherwise, all references to fat will be to the true chemical term, triglyceride.

Interstitial lipid will be expressed as a percentage of muscle mass, not total body mass or total fat mass.

1.3 Lipid vs. Adipose Tissue

Another common terminology error associated with "fat" is the difference between lipid and adipose tissue. The human body can be sub-divided into hierarchical levels, each with its own qualities (Wang *et. al.*, 1992). Many researchers equate adipose tissue with lipid, though the former is a tissue while the latter refers to molecular components of the body. Adipose tissue is not only the cellular triglyceride and lipids, but also contains cellular components such as cytosol, mitochondria, the Golgi apparatus, nuclei, membrane lipid and fibrous matrix supporting the cells. The difference is subtle, but the lipid component of adipose tissue can be quite

variable, as demonstrated in two cadaveric studies. Forbes *et. al.* (1953) and Forbes *et. al.* (1956) demonstrated in three cadavers having percent body fat values of 4.32, 19.44, 27.93% had 4.24, 71.57, and 78.35% lipid respectively for actual adipose tissue composition.

Therefore care should be taken when using various techniques to quantify specific biological components to ensure that the measurements are made on the same hierarchical level; otherwise assumptions or conversion formulas must be used to make the findings equivalent (Wang *et. al.* 1992).

1.4 Comparing MRI & Densitometry Results

Densitometry is a body composition technique capable of estimating total body fat by estimating lipid at the molecular level. When calculating total body fat, densitometry uses the density of triglyceride, 0.90 g/ml. This calculation is based on the assumption of constant lipid density, and that triglyceride occupies the majority of the human body lipid reservoirs (Siri, 1956; Fessenden *et. al.*, 1990).

MR technology quantifies body fat at either the atomic or the tissue level, depending on the method used. If the method is based on quantifying a signal intensity, the atomic level is being assessed. This is because each hydrogen atom involved contributes to the total signal output, so proton densities of specific components must be taken into account. If the analysis focuses on pixel intensity, area, or volumes, then it is adipose tissue that is

being imaged. Therefore, to compare MRI with densitometry, a conversion formula must be used to arrive at common values for either technique.

Based on the method used for this study, adipose tissue area and volume were determined from the MR scans. The adipose tissue volume was then converted to adipose tissue mass by assuming a constant density. Though the composition of adipose tissue has a significant range (Forbes *et. al.*, 1953; Forbes *et. al.*, 1956; Martin *et. al.*, 1985), Thomas (1962) and Pawan *et. al.*, (1960) arrived at 85% average lipid content. This value was used to convert adipose tissue mass to a lipid mass. If the actual adipose composition values paralleled the extreme values of Forbes *et. al.* (1953), Forbes *et. al.* (1956) and Thomas (1962), then an error in the interstitial lipid value would be introduced. This error, based on the extreme values of 61.0% and 94.1% lipid would generate an error of –27% and +10.5%. The value of 4.24% (Forbes *et. al.* 1956) for the lipid fraction of adipose tissue was not used as an extreme value because Forbes *et. al.* (1956) described the cadaver as being unusually "wet" possibly due to the IV fluids infused prior to death. The final result of the conversions was a MRI value expressed as lipid mass which can be compared to total body fat or muscle mass.

One major drawback of hydrostatic weighing is that it is not capable of discerning individual lipid depots. This prevents densitometry from quantifying interstitial lipid solely, therefore MR imaging is conveniently used to assess the interstitial site.

1.5 Purpose

The purpose of this study was three-fold:

- 1) To quantify interstitial lipid at twelve selected limb segment sites *in vivo* using magnetic resonance imaging.
- 2) To compare the value of interstitial lipid determined by MRI with total body fat, determined from densitometry.
- 3) By quantifying interstitial lipid at three consecutive sites on a limb segment, assess interstitial lipid's variability intra- and intersegmentally.

1.6 Research Hypotheses

Though previous cadaver studies have had small sample sizes, two general hypotheses were proposed for the MR-determined interstitial data:

- 1) Interstitial lipid occupies a greater percentage of the interstitial compartment in higher total body fat individuals than in leaner individuals.
- 2) Interstitial lipid will remain relatively constant throughout the various sites.

CHAPTER 2

REVIEW OF LITERATURE

PART I – DENSITOMETRY & INTERSTITIAL LIPID

Prior to 1942, methods to quantify lipid *in vivo* were limited, and typically involved only simple mathematical and geometric models and accepting several assumptions whose validity were questionable. Behnke (1942) devised densitometry, a mathematical model with various assumptions, capable of indirectly estimating total body lipid *in vivo*. Since its inception, densitometry has been regarded as a reference method for *in vivo* body fat determination.

2.1 Densitometry

2.1.1 Theoretical Principles of Densitometry

In an attempt to quantify lipid *in vivo*, Behnke (1942) devised an indirect protocol, densitometry (or underwater weighing or hydrostatic weighing). It views the human body as being comprised of two-compartments (lipid and non-lipid) and assumes a constant density of these two compartments to arrive at a value of percent body fat by mass.

Densitometry utilizes Archimedes Principle of water displacement, and its relationship to density, mass, and volume to determine total body density

(Behnke, 1942). Mass is determined by weighing the subject in air. By Archimedes Principle, the volume of the subject is equivalent to the mass of water displaced. The volume of the water displaced may be measured by a manometer or by measuring the buoyant force acting on the submerged body (Behnke, 1942). The buoyant force acting on the subject is equal to the mass of the water that it displaces. Since the density of water is 1.00 g/ml, the volume of water is equivalent to the mass. Therefore, the volume of the submerged subject is known. Volume is corrected for the residual volume of air left in the lungs after forceful exhalation, volume of gas in the gastro-intestinal tract and adjusting for the density of water at the current water temperature and barometric pressure. This data will yield a density for subject.

To arrive at a percent body fat from the density, the body must be viewed as a two compartment model: a lipid compartment and a lipid-free compartment. Several assumptions must be made regarding these compartments (Allen *et. al.*, 1959; Siri, 1956; and Brozek *et. al.*, 1963)

- the density of the lipid compartment is known and constant.
- the density of the non-lipid compartment is known and constant.
- the components of the non-lipid compartments normally exist in constant proportions.
- the hydration of the lipid-free component is constant.

2.1.2 Assessment of Densitometry Assumptions

The lipid compartment of the body consists primarily of triglyceride (Fessenden *et. al.*, 1990) which has a constant density of 0.90 g/ml. Small quantities of other lipid exist in the body, such as phospholipids and cholesterol, which have densities greater than 0.90 g/ml but their relatively small quantity has little effect upon the density of total body lipid (Brozek *et. al.* , 1963). Thus the density of the lipid compartment is readily accepted at 0.90 g/ml.

The assumptions of a constant and known density for the non-lipid compartment are more questionable than the assumption for a constant lipid density. The density of the lipid-free compartment is assumed to be 1.1 g/ml (Siri, 1956), which is a combined value of the lipid-free components, primarily muscle and bone.

Fresh, lipid-free skeletal muscle density has been quantified at 1.062 g/ml (Mendez *et. al.*, 1960), and 1.066 g/ml (Forbes *et. al.*, 1953). Allen *et. al.*, (1959) determined a lipid-free skeletal muscle density of 1.07 g/ml. It is assumed to be relatively constant based on the limited preceding data (Mendez *et. al.*, 1960; Forbes *et. al.*, 1953; Allen *et. al.*, 1959).

Several studies have indicated that bone mineral density has a greater variability. Table 2.1 displays the results of several cadaveric studies that determined the density of bone. Siri (1956), Bakker *et. al.*, (1977), and Lohman

(1981) estimated that the variability in bone mineral density could result in a theoretical error of 3-4% for predicting body fatness.

Table 2.1: Density of bone tissue in cadaveric subjects determined by various researchers.

Researcher	Bone Density Range (g/ml)	Fresh or Fat-Free Bone
Leusink (1972)	1.25 - 1.30	Fresh Cadaver
Bakker & Struikenkamp (1977)	1.22 - 1.30	Fresh Cadaver
Martin & Drinkwater (1991)	1.18 - 1.33	Fresh Cadavers
Martin & Drinkwater (1991)	1.43 (calculated value)	Fat-free Bone

Fuller *et. al.* (1992) used both individual and multi-component methods to estimate various parameters, including percent body fat and the density of the lipid free mass in twelve female and sixteen male subjects. Ages, mean (SD), of the subjects were 31.8 (11.0) and 33.8 (10.7) years old for the females and males, respectively. Fuller *et. al,* .(1992) estimated the density (mean (SD)) of lipid-free mass to be 1.1003 (0.0066) kg/L and 1.1024 (0.0078) kg/L for women and men, respectively, with no significant difference between the two. The hydration fraction of the fat-free mass was calculated to be 0.7449 (0.0192) and 0.7332 (0.0219) for females and males, respectively. If the extremes were used, it would result in a 25% error in the fat estimation, though Fuller *et. al.* (1992) deemed the assumed value of 1.1 g/ml for Siri's (1956) densitometry equation to be appropriate if not applied universally, such as for osteoporotic or edematic subjects.

The assumption that bone and muscle normally exist in constant proportions is critical in determining body density, but its validity is limited. Martin *et. al.* (1991) measured that the percentage of lipid-free muscle in the adipose-free mass ranges from 40-60 % with a mean of 50%, with bone ranging from 16.3 to 25.7% of the adipose-free mass. The four cadavers in the studies of Mitchell *et. al.* (1945), Forbes *et. al.* (1953), and Forbes *et. al.* (1956), demonstrated the percentage composition of the fat-free mass ranged from 34.9-50.6% for fat-free muscle and 14.1-16.4% for fat-free bone. Changes from the assumed proportion in a subject result in the density of the lipid-free mass diverging from the assumed 1.1 g/ml. This may result in an over or under-estimation of body fat for the individual. Siri (1956) concluded that the variability in protein:mineral ratio could lead to a variation in percent body fat of 2.1%. Bakker *et. al.* (1977) suggested a standard deviation of 0.01 g/ml for the density of the fat-free mass, with Martin *et. al.* (1991) estimating it may be as high as 0.10 g/ml. The difference between the assigned and actual density of the fat-free mass in a given individual of as little as ±0.02 g/ml produces an error for estimated fat percentage in the order of ±7% fat.

2.1.3 Density to Percent Fat Conversion Formulas

Siri (1956) and Brozek *et. al.* (1963) have developed formulas for converting the body density determined by hydrostatic weighing to a value of percent fat. Both of these formulas are fundamentally the same

mathematically, but differ in the values assigned to the density of the fat and the fat-free mass.

The conversion formula of Siri (1956) is derived from the assumed values of lipid density (0.90 g/ml) and non-lipid compartment density (1.1 g/ml). This formula is accepted as a reasonable estimate and has been in use since its inception:

Fat Mass (kg) = (4.95/Density) – 4.5

Brozek *et. al.* (1963) derived a similar formula to that of Siri's (1956), but based it on experimental "real-life" evidence. Brozek *et. al.* (1963) reviewed the research of Forbes *et. al.* (1953), Forbes *et. al.* (1956) and Mitchell *et. al.* (1945) to produce a reference body, which had slightly different values for the lipid and non-lipid density. The resulting formula produced by Brozek *et. al.* (1963) was:

Fat Mass (kg) = (4.57/ Density) – 4.142

2.1.4 Densitometry's use in the field of Body Composition

Recently, densitometry has been used extensively as one method in combination with others to form multi-component techniques (Fuller *et. al.*, 1992; McNeill *et. al.*, 1991; Heyward, 1996). Densitometry is used as a criterion method to determine body density; this is performed in conjunction with other techniques involved in the multi-compartment models.

Research strongly suggests that multi-component models be used in body composition assessments of population subgroups, that may not conform to the density-to-fat conversion formulas of Siri (1956) and Brozek *et. al.* (1963). The formulas of Siri (1956) and Brozek *et. al.* (1963) have been derived from direct analysis of Caucasian male and female cadavers, who were not necessarily representative of a substantial proportion of the population including different ethnic and age subgroups. The theory behind multi-compartment models is to reduce the error associated with any one technique for assessing various compartments.

Fuller *et. al.*, (1992) assessed body composition *in vivo* comparing a four component model of body composition with the individual reference methods (densitometry, deuterium dilution, dual energy x-ray absorptiometry (DEXA), whole-body ^{40}K) and "bedside" methods (skinfolds and bioelectric impedance). Results indicated that DEXA predicted multi-compartment determinations slightly less well than deuterium dilution or densitometry, presumably because of the great influence these methods have on the multi-compartment model. Fuller *et. al.* (1992) and Kohrt (1995) indicate that body composition testing on Caucasian males with underwater weighing does not differ significantly from multi-component results. This suggests that body fat testing on populations similar to those of Siri (1956) and Brozek *et. al.* (1963) may be performed with underwater weighing without introducing significant error.

McNeill *et. al.* (1991) compared six methods (densitometry, body-water dilution, whole-body counting (^{40}K), skinfold thickness, bioelectric impedance, and magnetic resonance imaging) of determining body fat; densitometry was considered the criterion method. MRI had the lowest variability in difference from underwater weighing estimates of body fat (2.3% SD(2.9%)), suggesting that MRI may be a satisfactory substitute for underwater weighing.

2.2 Interstitial Lipid

Few studies have quantified interstitial lipid in cadaveric specimens in the past, with the majority of research coming from four studies in the middle half of the twentieth century.

Mitchell *et. al.* (1945) quantified interstitial lipid *in vitro* in one cadaver, a Caucasian thirty five year old male. The cadaveric specimen was dissected and representative samples of the major tissues were selected for composition testing. Lipid quantification was performed using chemical extraction technique. Interstitial lipid occupied approximately 3.35% of the skeletal muscle tissue (Table 2.2).

Forbes *et. al.* (1953), performed body composition analysis on a Caucasian forty six year old male. Composition analysis followed the technique of Mitchell *et. al.* (1945). Interstitial lipid comprised approximately 6.60% of the skeletal muscle (Table 2.2).

The research of Forbes *et. al.* (1956) involved complete body composition analysis on two cadavers; a sixty year old Caucasian male and a forty eight year old African-American male. The body composition methodology followed that of Mitchell *et. al.* (1945) and produced values of 9.4% interstitial lipid from the Caucasian cadaver and 2.22% interstitial lipid of the African-American cadaver (Table 2.2).

Moore *et. al.* (1968) performed both antemortem and postmortem body composition analysis on a sixty seven year old female to validate various isotope dilution methods against direct tissue assessment. Though Moore et. al (1968) primarily focussed on skeletal assessment, though adipose and muscle tissue were also analyzed. The skeletal and muscle tissue were isolated and pulverized for analysis. Direct composition analysis indicated 16.2 % total body fat, 23.13% muscle with fat occupying 2.9 % of the muscle (interstitial lipid), summarized in Table 2.2.

Table 2.2: Tissue distribution in 5 cadavers.

	Mitchell *et. al.* (1945) †	Forbes *et. al.* (1953) †	Forbes *et. al.* (1956)*†	Forbes *et. al.* (1956)**†	Moore *et. al.* (1968) ‡
Age:	35	46	60	48	67
Total Body Mass (kg):	70.55	53.8	73.5	62.0	43.4
Total Body Fat (%):	13.63	11.37	21.67	5.18	9.36
Muscle (%):	31.56	39.76	40.22	42.53	23.13
Interstitial Lipid (% Skeletal Muscle):	3.35	6.60	9.40	2.22	2.9
*Caucasian **African-American	† male ‡ female				

The data from Table 2.2 indicates interstitial lipid ranges from 2.22-9.4% in representative samples of skeletal muscle mass.

Mendez *et. al.* (1960) determined a value of 2% for intramuscular lipid on small mammals using chemical extraction. This value may be artificially low because the visible adipose was stripped away from the muscle tissue.

PART II - NUCLEAR MAGNETIC RESONANCE SPECTROSCOPY& MAGNETIC RESONANCE IMAGING

The physical process of Nuclear Magnetic Resonance (NMR) was first recognized in 1946 (Bloch, 1946; Purcell *et. al.*, 1946), but was not readily accessible as a chemical analytical tool until the advent of Fourier transform NMR (Ernst *et. al.*, 1966) twenty years later. NMR is still used as a chemical analytical tool (Oldendorf *et. al.*, 1991) to identify isolated or purified organic compounds according to the unique hydrogen spectrum that they produce. In about 1976, NMR was adapted to produce images which were applicable in a medical setting. These first imaging tools were termed NMR scanners, though the term "nuclear" was not eagerly accepted among the public with its association to radiation, so the term Magnetic Resonance Imaging (MRI) was adopted (Oldendorf *et. al.*, 1991; Garlick *et. al.*, 1992).

MRI employs the same physical principles of NMR but "refers to the process of exploiting NMR to make medical images in a clinical setting" (Oldendorf *et. al.*, 1991). Lay people sometimes confuse MRI with CT scanning, though the two methods are based on very different scientific principles.

2.3 Magnetic Resonance Imaging

To be susceptible to MRI, an element must have a magnetic field or dipole. Of the approximately 280 stable nuclei, 100 have magnetic dipoles. This dipole exists in elements with an unpaired proton, neutron, or both (Oldendorf *et. al.*, 1991). Of all magnetic nuclei, hydrogen is of the greatest biological interest because it occupies two-thirds of the atoms in biological tissues, and partly because it is extremely magnetic (Dixon, 1984; Oldendorf *et. al.*, 1991; Hashemi *et. al.* 1997). Hence, MR imaging of the hydrogen atoms within an object is sometimes referred to as proton imaging.

Though the nuclear physics to produce an image from the concept of magnetic resonance is complex, the basic principles of NMR and MRI are straight-forward. The hydrogen nuclei in the body are dipoles and under normal conditions they align randomly, so the body has no net magnetic field. When the body under investigation is placed within a large magnetic field (B_o), the hydrogen nuclei align with or opposed to the field, producing a net magnetization (M_o). The nuclei precess about the axis of the magnetic field with a given resonance frequency (the Larmour frequency), which is proportional to the external magnetic field strength (B_o). If a radiofrequency (RF) pulse corresponding to the Larmour frequency is then applied in a perpendicular plane (a 90° pulse) to the magnetic field, the nuclei are perturbed from their aligned direction with the magnetic field. When the stimulatory RF pulse is stopped, the nuclei oscillate back to align with the

magnetic field in a lower energy state and release an RF signal, termed Free Induction Decay (FID), based upon their chemical environment. This RF pulse is detected by the receiving coil and processed into an image.

Clinicians take advantage of the properties of different tissues and bodily fluids to produce different images. This is done by altering the repetition time (TR) or echo time (TE) of a pulse sequence to enhance a desired tissue or fluid structure; this is termed T_1 or T_2 weighting.

To comprehend the significance of these terms, their definitions are provided.

- T_1 Relaxation Time: is the time it takes for the hydrogen nuclei to emit 63% of the energy they absorbed from the stimulatory pulse.
- T_2 Relaxation Time: is the time it takes for 63% of the signal to be lost due to dephasing.
- Repetition time (TR): refers to time duration between RF stimulatory pulses.
- Echo Time (TE): the time between the end of the stimulatory pulse and when the receiving coil detects the FID.

An example of a repetition time denoting a T_1 weighted scan is a TR of 500 ms. The chemical environment of a group of nuclei will dictate how quickly the nuclei release their energy in the RF pulse (Oldendorf *et. al.*, 1991; Hashemi *et. al.* 1997). Aliphatic nuclei of lipid molecules release their RF

pulse very quickly (<500 ms); therefore these nuclei have released all of their energy and will accept the full energy of the next repeated pulse (Oldendorf *et. al.*, 1991). These nuclei fully contribute to the image and the fat will appear very bright in the image. Cerebrospinal fluid (CSF) does not release the energy quickly (>2000 ms) and therefore does not absorb a lot of the repeated stimulating RF pulse. Therefore, with repetition time of 500 ms, CSF appears dark. Because a 500 ms TR affects the contrast, this pulse is considered T_1 weighted (Oldendorf *et. al.*, 1991; Hashemi *et. al.* 1997).

When reference is made to T_2 weighting an image, the pulse sequence has been designed so that the TR is large enough (> 2000 ms) to have little effect upon the brightness contribution of tissues to the image. This is because all the tissues have released most of their energy by the time the next stimulatory pulse, so all the tissues fully absorb the energy of the next stimulatory pulse. Therefore, TR has little effect on the contrast of the tissues. To obtain sufficient contrast then, a short spin-echo (TE) is used.

By altering TR and TE, a conventional MR image can enhance certain tissues and produce the desired image for clinical use.

2.4 Chemical-Shift Imaging

It is important to differentiate between magnetic resonance imaging and its subdiscipline, chemical-shift imaging. In conventional proton MRI, no distinction is made with regard to the chemical environments associated

with the various hydrogen atoms in the body (Brateman, 1986; Buxton *et. al.*, 1986; Bax *et. al.*, 1986). Chemical-shift imaging uses the small differences in resonance frequency of different chemical species to generate images of particular species.

Determining the spatial distribution of nuclei that have a particular resonance frequency, such as water protons, rather than imaging the entire spectrum of resonance frequencies within a scanned area is chemical-shift imaging (Brateman, 1986). This technique allows for the observation of a specific portion of resonance frequencies, which allows lipid to be discriminated from water (Dixon, 1984) and even individual metabolites to be detected, identified and possibly quantified in vivo (Iles *et. al.*, 1982; Radda, 1986; Iles *et. al.*, 1988).

The differences in resonance frequency between different chemical species is a result of the chemical environment surrounding the hydrogen nuclei. The long carbon chains of lipids shield the bound hydrogen nuclei differently than the oxygen atom of the water molecule, so the signal that these molecules produce is "shifted" by several part per million (ppm) on chemical spectra and can therefore be differentiated. This principle of chemical-shifts has been the foundation of NMR and has been utilized extensively in spectroscopy for many years, but only recently has technology applied chemical-shifts to imaging techniques.

Many pulse sequences have been developed that utilize the differences in resonance frequency to preferentially image a specific class of molecule. These techniques include selective excitation, selective suppression and various other modified CSI techniques.

Selective excitation methods use a RF pulse that excites a narrow range of frequencies exclusively. Suppression methods are based on imaging a specific portion of frequencies by saturating unwanted frequencies with the application of an excess radio frequency pulse prior to the data acquisition pulse sequence (Bottomley *et. al.*, 1984). This is dependant on T_1 relaxation time of the resonance of a particular species. These techniques have been effective to image lipid or water exclusively in several tissues (Bottomley *et. al.* , 1984; Pykett *et. al.*, 1984; Rosen *et. al.* , 1984; Frahm *et. al.*, 1985; Haase *et. al..*, 1985; Matthaei *et. al.* , 1985).

Modified chemical-shift techniques (Sepponen *et. al.*, 1984; Dixon, 1984) acquire several images at specific times after the data acquisition pulse is applied. The images produced have different types of tissues highlighted because the images are collected at different points in time on the FID. Dixon (1984) devised a CSI protocol to produce images of water and lipid, which was demonstrated on various lipid and water containing objects. Dixon (1984) used the difference in resonance frequencies of lipid and water at 0.35 Tesla (T) to produce two images: an in-phase "Water + Fat" image and an opposed "Water - Fat" image. When the maxima of the water and lipid signals

overlap, the in-phase image is generated; when the maxima of one overlaps the minima of the other, and opposed image is produced. These images could then be added or subtracted to produce a water or lipid image, respectively. Various studies have utilized Dixon's methodology to image lipid *in vivo* for clinical purposes, such as fatty liver disease (Lee *et. al.* , 1984 and Heiken *et. al.* , 1985). Buxton *et. al.* (1986) used Dixon's method to quantitatively determine the lipid content of phantoms containing 0-50% fat by weight and found that the fraction of lipid determined by CSI correlated well with the fraction determined by weight (r=0.995). Wong *et. al.* (1994) used a modified Dixon technique to compare the lipid determined by CSI in various fatty tissues with the lipid determined by chloroform extraction (r=0.99).

2.5 Quantification of Adipose Tissue and Lipid with MRI & CSI

Many researchers have adapted these MR methods and pulse sequences to not only image various chemical spectra, but to quantify various body components from the resulting spectral data.

One of these MR methods is the image segmentation method. The magnetic resonance image segmentation method is based on the concept that one could assign a threshold value to adipose tissue (AT) pixel intensity when imaged. The resulting image would then have highlighted adipose tissue pixels with intensities above this threshold and the water pixels would

appear dark. Several researchers (Staten *et. al.*, 1989; Gerard *et. al.*, 1990; Seidell *et. al.*, 1990; Ross *et. al.*, 1991; Ross *et. al.*, 1992; Ross *et. al.*, 1993; Roberts *et. al.* 1993; Abate *et. al.* 1994) have published studies in which MRI data was collected and analyzed by assigning AT thresholds which enabled the calculation of AT areas. These areas were then used to calculate AT volumes by multiplying the areas by MRI slice thickness to arrive at a volume. By combining multiple slices, regional and whole body adiposity could be estimated.

Staten *et. al.* (1989) measured the area of subcutaneous abdominal and visceral adipose tissue with three transaxial slices in each of six subjects (three male, three female) using an AT threshold technique. They used a 500 ms TR and a 17 ms TE with a 1.5T magnetic field. The subcutaneous and visceral values were compared with total body fat, which was determined using hydrostatic weighing using the conversion formula of Brozek *et. al.* (1963). Staten *et. al.* (1989) indicated that total abdominal and subcutaneous abdominal fat areas by MRI correlated closely with percent body fat by hydrostatic weighing ($r = 0.95$ and 0.98, respectively).

McNeill *et. al.* (1991) determined total body fat in seven lean and seven obese women using six methods, including underwater weighing (UWW) and an image segmentation MR method. A fast inversion recovery pulse sequence was used at 0.08 T to provide good discrimination between adipose and lean tissues. The MR data showed the lowest variability in difference

from underwater weighing (2.3 (SD 2.9)%), indicating that the MR image segmentation method can provide a similar estimate of total body fat to densitometry.

Fowler *et. al.* (1992) validated the use of an MRI image segmentation method against direct dissection and lipid chemical analysis to quantify AT in pigs. The pigs were scanned, sacrificed and subsequently dissected. A total of thirteen scans were made with four image types (inversion recovery [IR], proton density [PD], spin lattice relaxation T_1, and "difference" [PD-IR]) produced. The adipose tissue was then quantified using an image segmentation method described in Fowler *et. al.* (1990) and Knight *et. al.* (1990). The resulting values were expressed as a proportion of the total adipose. The dissected adipose tissue was weighed to determine its mass. Chemical lipid extraction was performed on the homogenized tissues once the carcass was ground up using the methanol-chloroform technique described by Atkinson *et. al.* (1972). Fowler *et. al.* (1992) indicated that total percent lipid was closer to percent adipose determined by MRI (1.2% overall difference) than between total lipid and total adipose as determined by dissection. Correlations between adipose distribution measured by MRI and dissection (r=0.980) or MRI and chemical analysis (r=0.979) were similar to that between dissection and chemical analysis (r=0.995). Fowler *et. al.*'s (1992) study indicates that the image segmentation MR technique produced accurate estimates of percent adipose tissue.

Ross *et. al.* (1992) assessed total and regional adipose tissue by volume *in vivo* using MR image segmentation and compared these results with selected anthropometric variables. The MR pulse sequence was a 500 ms TR with a 20 ms TE on a 1.5 T Philips whole body scanner. Forty-one scans were taken on each of twenty seven healthy males. The adipose tissue was determined using a threshold of 110 out of 256. This threshold value was arrived at through "the analysis of a sample of typical images and the respective gray level histograms" (Ross *et. al.*, 1992). Therefore, all pixels above this intensity were considered adipose tissue. Adipose tissue volume was determined for each slice and a total calculated through linear interpolation. The adipose tissue was categorized as subcutaneous or visceral. Visceral adipose tissue accounted for 18% of the total adipose tissue volume. Ross *et. al.* (1992) indicated the single best anthropometric predictor of total adiposity was waist circumference ($r = 0.96$).

Ross *et. al.* (1993) measured subcutaneous and visceral adipose tissue area and volume in obese women using their previously published imaging protocol (Ross *et. al.*, 1991). Large interindividual differences were observed for both adipose depots. Ross *et. al.* (1993) indicate that subcutaneous and visceral adipose tissue represented 94% and 6% of the total adipose tissue volume, respectively, with bone marrow and interstitial adipose not considered.

Abate *et. al.* (1994) validated the quantification of adipose tissue by mass in the subcutaneous and intra-abdominal compartments using MRI against dissection on three unembalmed cadavers. For the various compartments measured, the mean of the difference between the two methods was only 0.076 kg. The limits of agreement between the two techniques were -0.066 kg and 0.218 kg. The results indicated that MRI was a precise and accurate method for determining adipose tissue mass in these two compartments.

2.6 Spectral Imaging of Interstitial Lipid *in vivo*

Many studies have imaged the spectra associated with skeletal muscle tissue, but few have quantified the lipid within skeletal muscle.

Narayana *et. al.* (1988) imaged the spectra of the gastrocnemius muscle from twelve normal volunteers using a depth-resolved surface coil spectroscopy technique (DRESS) described by Bottomley *et. al.* (1984). The spectra imaged on two different occasions from the same individual exhibited very little variation. With regards to interindividual differences, Narayana *et. al.* (1988) indicated that gross spectral differences do not appear between individuals but the number and relative amplitudes of the resonances from the fatty acid chains do appear to have significant variation. This suggested that there may be significant variation in the lipid composition between individuals, but because the two spectra from one individual are consistent, the progress of changes may be monitored.

Bruhn *et. al.* (1991) used a chemical-shift selective (CHESS) method to image the spectra of volumes-of-interest (VOI) in the quadriceps muscles *in vivo*. The resulting lipid spectra changed when the VOI was shifted even slightly. Bruhn *et. al.* (1991) indicated that spectra exhibited remarkable intra and interindividual differences in the absolute signal intensities of mobile lipids. These results suggest that intramuscular lipid quantities may change from site to site.

Schick *et. al.* (1993) used CSI to image and observe spectra of intramuscular lipid *in vivo*, but did not quantify the lipid in the scanned region. They used a double spin echo (PRESS) localization technique to compare volume selective spectra of lipid in the human soleus muscle, subcutaneous adipose tissue and yellow bone marrow. Schick et. al (1993) selected a region within the muscle belly not associated with the septa because the lipid in this area satisfied his criteria of homogeneity. The resulting spectra indicated that the soleus lipids were of similar composition, but were compartmentalized because of the shift in Larmour frequency. Schick *et. al.* (1993) believed this was due to the lipids being intracellular or extracellular.

2.7 Quantification of Interstitial Lipid *in vivo*

In 1997, a study by Leroy-Willig *et. al.* (1997) performed body composition analysis using an MR image segmentation method to quantify lipid (interstitial and subcutaneous) in boys ages 9-12 with Duchenne

muscular dystrophy (DMD) and controls. Sixty images were taken from ankles to jaws at a slice interval of 20mm using a pulse sequence of 600 ms TR and 20 ms TE; this was altered when scanning the thorax to compensate for respiratory artifacts. Twelve reference images were used to compartmentalize the lipid. By extrapolating the lipid values for the twelve slices a total interstitial lipid mass was arrived at. Interstitial lipid mass was determined to be (mean (SD)) 4.9 (2.4) kg for the DMD boys and 0.6 (0.4) kg for the controls; these are significantly different ($p<0.001$).

2.8 Summary

The spectral results are somewhat contradictory regarding intra-individual variations. Therefore it is difficult to generalize the findings because spectral data from intramuscular images are taken from such a very small volume and there is no quantitative analysis.

The study of Leroy-Willig (1997) provides a baseline quantity for total interstitial lipid based on twelve scans. Little is still known regarding intra-individual differences for interstitial lipid or how it varies with accurate estimates of total body fat.

CHAPTER 3

METHODS

3.1 Subjects

Twenty, healthy, Caucasian males between the ages of 19-29 years old were recruited on a volunteer basis using several posters located on the University of Calgary campus. To ensure a wide range of total body fat, subjects were initially screened using Parizkova's (1978) anthropometric method and equation. Subjects were viewed as conforming to one of three categories of total body fat: 1) < 12 % 2) 12-16 % 3) > 16 %, so that a wide spectrum of subjects may be selected that represent the general population. Subjects were then selected at random from the categories for testing. Subjects were excluded from the study if they did not meet the exclusion criteria (Appendix B) for MRI. Subjects were asked not to exercise immediately prior to or between MRI and densitometry testing sessions. Ethics approval was granted by the Center for Advancement of Health and the Medical Bioethics Committee; informed consent (Appendix C) was provided by all subjects.

3.2 General Methodology:

To randomize data collection, MRI and densitometry times were scheduled in an alternating arrangement and selected subjects were randomly

assigned to a time. The following description of the methodology was based on a subject randomly assigned to partake in the MRI portion prior to the densitometry/anthropometry testing.

The subject arrived at the MRI Center in Foothills Hospital in Calgary, Alberta, Canada, and privately changed into a T-shirt and shorts so accurate landmarking of the selected sites for MRI scanning could be performed. This attire also maximized the subject's comfort during the testing. MRI scan order of each limb segment was randomly determined and the basic MRI procedure was reviewed and any final questions were answered. The scans were then performed, with the entire procedure taking between forty-five minutes to one hour. The subject reported to the Human Performance Laboratory at the University of Calgary for densitometry/anthropometry testing the next day (within 24 hours).

At the Human Performance Laboratory, the subject was given a review of the densitometry, residual volume, and anthropometric procedures. The subject's muscle mass was first assessed according to Martin *et. al.*'s (1990) anthropometric protocol, followed by underwater weighing and residual volume testing. This portion of the testing lasted approximately one hour.

3.3 Specific Testing Protocols

3.3.1 Magnetic Resonance Imaging Methods

The General Electric 1.5 Tesla SIGNA whole body scanner (General Electric Medical Systems, Milwaukee, WI) in the Magnetic Resonance Imaging Center at Foothills Hospital in Calgary, Alberta, Canada, was used to collect the MRI data.

The order of scanning for the limb segments was randomized. Twelve, 20 mm thick scans were made on each subject at the following sites:

- Upper Arm, 3 sites: Maximum girth, and proximal/distal 2 cm.
- Forearm, 3 sites: Maximum girth and proximal 2 and 4 cm.
- Upper leg, 3 sites: Mid-Thigh, and proximal/distal 2 cm.
- Lower leg, 3 sites: Maximum girth, and proximal/distal 2 cm.

The maximum girths and thigh mid-point were used as reference points for the three slices. These reference points were used by anthropometric convention and were easily landmarked using a metric tape measure. By anthropometric convention, all measurements were taken on the right side of the body.

The subject was then positioned in the scanner to acquire data from the randomly selected limb segment. For upper limb measurements, the subjects were inserted into the General Electric 1.5 Tesla SIGNA whole body scanner in a head-first prone position with arms raised above the head to permit entry into the bore. Subjects were positioned on their back and feet first for all

lower limb measurements. These were the most comfortable positions that allowed accurate scanner landmarking of the reference sites. The reference landmark was positioned in the isocenter of the imaging planes. Because the sites on each limb segment were consecutive and in the same plane, all data from the three sites on a limb segment was collected simultaneously. Each limb segment had a scan time of approximately four minutes and twenty seconds. Between each scan series, the subject was allowed to sit up and stretch before the next limb segment was scanned.

A pulse sequence with a repetition time of 500 ms and an echo time of 17 ms was used for all acquisitions, with images acquired on a 256 x 256 matrix within a 24 cm field-of-view (0.88 m m^2 pixels) with two excitations per scan. Three, 20 mm transverse slices were imaged per limb segment. Additional superior and inferior saturation pulses were applied prior to the stimulatory pulse sequence to eliminate an image artifact due to blood flow. The data was collected using a transmission-receiving extremity surface coil which encompassed the selected portion of the limb segment. In applicable scenarios, an "offset" was used to provide the subject with a suitable scan position and comfortable entry into the bore. "Offsetting" refers to shifting the extremity surface coil off of the isocenter of the magnet; a gradient pulse is then applied to the pulse sequence to obtain the proper spatial image and data.

This data was then transferred from Foothills Hospital Computer System to the Human Performance Laboratory at the University of Calgary using the file transfer protocol (FTP) of the telnet computer system.

3.3.2 Densitometry Methods

Within 24 hours (either preceding or following) of the MRI data collection, the subjects had their total body fat estimated by hydrostatic weighing using the densitometry tank (developed by the Faculty of Engineering, University of Calgary) at the Human Performance Laboratory, Faculty of Kinesiology, University of Calgary. The protocol used was originally developed by Behnke (1942).

Immediately prior to a subject's testing, the weight of the suspended seat with the weight belt, along with the water temperature and barometric pressure were determined. Water temperature was kept at approximately 34° Celsius for subject comfort. The subject's weight in air was determined prior to underwater weighing.

The subject, wearing a bathing suit and the attached weight belt, entered the tank and ensured all air bubbles clinging to their body and bathing suit had been removed. The subject perched on the suspended platform, quietly submerged and released all air from their lungs while crouching into a squat position to aid in the evacuation of air from their lungs. When evacuation was complete and the digital scale and strain gauge (OMEGA

Engineering Inc., Laval, QB; www.omega.com) stabilized, the value was recorded. This was repeated up to ten times for reliability and the mean of the three highest values accepted. Three researchers were present at all times to ensure that the subject was safe and comfortable. With underwater weighing complete, the subject's residual volume was determined.

3.3.3 Residual Volume Methods

Residual volume was determined using a slightly modified Wilmore *et. al.* (1980) oxygen dilution method.

Upon arrival at the Human Performance Lab, the initial test was to determine vital capacity using a Collins Eagle One spirometer (Bionetics Ltd., Markham, ON). With vital capacity known, the appropriate sized (five or seven litre) anaesthetic bag could be selected for residual volume testing.

The correct anaesthetic bag was filled to approximately 105% of the subjects vital capacity to ensure the subject would never be deprived of air. This was filled by attaching the bag to the output valve of a vacuum pump (Harvard Dry Gas Meter, Collins Corp., MA) capable of measuring the amount of air expelled and attaching the oxygen cylinder to the intake port. The volume of oxygen was measured to the nearest 0.1 L.

To ensure 100% oxygen in the bag, two safeguards were introduced into the procedure.

1) The bag was flushed three times with pure oxygen before the final filling.

2) Prior to opening the T-valve to the anaesthetic bag, it was capped and the oxygen turned on. This produced a positive pressure in the output hose. The cap was then removed, the pressure released, and the T-valve was immediately turned to access the bag. This helped limit any room air contamination.

The bag and T-valve was disconnected from the vacuum and a mouthpiece attached to one of the ports on the T-valve. This apparatus was then extremely mobile and was carried up the stairs of the underwater weighing tank to the awaiting subject. The procedure for the residual volume testing was then explained to the subject and any questions were answered. The subject remained in the underwater weighing tank submerged up to the neck to reproduce the pressure exerted on the lungs by the water. To accommodate this position, the subject stood on a collapsible seat built into the structure of the tank.

With a researcher holding the T-valve and bag apparatus to prevent any potential drowning incidents, the subject inserted the mouthpiece and applied a nose clip to produce a potentially closed system. The subject inhaled regularly five to six times with the T-valve positioned so the subject was exposed to room air, at which point the subject exhaled maximally, and raised their legs to aid in the evacuation. When the subject deemed that they had

exhaled maximally, the subject turned the T-valve to access the bag of 100% oxygen. This created the closed system needed for residual volume testing. The subject took five to six slow, successively deeper breaths. After about six breaths, the subject again exhaled maximally into the bag while bringing up their legs and the T-valve was closed off. The subject was then exposed to room air again and the apparatus was removed from the underwater weighing tank for gas analysis.

Gas analysis was performed on a Metabolic Measuring Cart (MMC) (MMC Horizon™ System, SensorMedics, Anaheim, CA). Prior to connecting the apparatus to the inspired port on the cart, the bag was shaken to mix the contents and approximately one liter of the gas was released by opening a stop-cocked line attached to the bag port on the T-valve. With one liter of gas removed and the MMC calibrated, the stop-cock was attached to the inspired port of the cart and the gas analyzed. The MMC was calibrated using a standard gas of 96% oxygen and 4% carbon dioxide, prior to every residual volume test. Gas analysis produced values for percent oxygen, carbon dioxide, and nitrogen.

This procedure was performed at least three times for each subject to ensure reliability of the measurements.

3.3.4 Anthropometric Methods

All subjects were measured to estimate regional skinfold thickness and muscle mass according to the procedure and sites described by Martin *et. al.* (1990). A series of ten measurements were taken including mass, height, girths, and skinfold thicknesses. All reference sites (maximum upper arm, maximum forearm, mid-thigh, and maximum calf girth) were landmarked according to anthropometric procedure (Appendix D) and subsequent sites were determined from these references sites. All skinfolds were measured using Harpenden calipers and girths measured using a metric tape measure. By anthropometric convention, all measurements were taken on the right side of the body and repeated up to three times to ensure their reliability.

3.4. Magnetic Resonance Image Analysis

3.4.1 Validation of Analysis

Like all scientific methods, the validity of the analysis had to be tenable. The greatest question of validity lay in the threshold value. Though the method itself is documented widely in the literature, it is not reasonable to simply use a threshold value from another researcher. This is due to the differences in data collection, different software and processes of analysis between researchers. The literature was consulted for the process of how researchers arrived at a threshold value, instead of the value itself.

Ross *et. al.* (1992) arrived at the threshold value through "the analysis of a sample of typical images and the respective gray level histograms". This process of choosing the threshold was similar to that described by Fowler *et. al.* (1990). This suggests that the scans and respective histograms were reviewed to arrive at a value for which the intensity corresponded to lipid. In this study, this technique was performed on approximately 130 scans to arrive at a threshold value of 195. Ross *et. al.* (1992) also described "ghosting", where an image artifact appears due to field inhomogeneities and the threshold had to be adjusted slightly; therefore the images in this study were visually reviewed for ghosting.

3.4.2 Analysis Methods

At the Human Performance Laboratory, the MRI raw data was analyzed on a Sun computer system. All raw data files had individual alpha-numeric codes, corresponding to the individual and the site; because the researcher was unaware of a particular subject's code, this enabled a blind analysis of the file without knowing the subject's total body fat. Each raw data file, which contained the three consecutive slices, was split into individual files using the computer program "rawmssplit" (Crawley, 1997), an in-house software package.

Each raw data file was processed through "rawnhtofold" (Crawley, 1995), an in-house software package, which changed the format from a

SIGNA file to a Float file with a 256 x 256 matrix so the files could be accessed by a subsequent computer program, "Viewdiff" (Chow & Smith, 1994).

The files were then transformed by "phasefit" (McGibney, 1992), an in-house software package, to correct for field inhomogeneities. This was accomplished by performing an Inverse Fast-Fourier Transformation (IFFT) and folding the image.

Image reconstruction was then performed in the program "Viewdiff Version 3.3" (Chow & Smith, 1992). "Viewdiff" (Chow & Smith, 1992) could reconstruct the real, imaginary, phase, and magnitude images from the raw data. By selecting the imaginary, IFFT, float image to be reconstructed, the success of the phase correction could be determined. If the phase correction was performed well, the imaginary IFFT float image has a centrally-located white pixel with a black background. Once this was ascertained, subsequent analysis could be done with "Viewdiff" (Chow & Smith, 1992).

The magnitude image was reconstructed in "Viewdiff" (Chow & Smith, 1992). Using the Colormap module of "Viewdiff" (Chow & Smith, 1992), the contrast and brightness were adjusted to 90 and 128, respectively, to give better contrast to the water and lipid-containing regions. The adipose tissue pixels were primarily bright and the water-containing pixels were dark. The image was then zoomed in 4x using the zoom bicubic interpolation feature in "Viewdiff" (Chow & Smith, 1992). With the image enlarged and quality preserved, the image was saved as a Sun Raster image using the

"Snapshot" tool in the Sun system. All images were transferred to an Apple Power Macintosh (Cupertino, CA; www.apple.com) via FTP to complete the image analysis using Adobe Photoshop 5.0 (Adobe Systems, CA; www.adobe.com).

On the Power Macintosh, the images were first converted from the Sun Raster format to TIFF using "Graphic Converter" (Lemkesoft, 1997; lemkesoft@aol.com). Images were opened using Photoshop and the subcutaneous adipose and bone regions were deleted to provide the interstitial area. A threshold was set at 195, with little variation occurring. This produced an image where pixels above this threshold (adipose) appeared white and pixels below this threshold (water) appeared black. Using the "histogram" command, the amount of adipose pixels and total number of pixels were determined, enabling a calculation for percent adipose tissue by area.

Because the MRI slices have a depth, the pixels can be thought of as voxels (the pixel area with a depth component determined by slice thickness), and can therefore be converted to volumes. Pixel area was determined to be 0.0088 cm^2 because the data was a 256x256 matrix with a 24 cm field-of-view (FOV). Voxel volume was therefore 0.0088 cm^2 x 2.0 cm. To convert the adipose tissue volume to a mass, a constant density was assumed as 0.9196 g/ml (Thomas, 1962). With an adipose tissue mass, the lipid mass could then be estimated based on the assumption that 85% of adipose tissue is

lipid (Thomas, 1962). The mean lipid mass for the three slices of each limb segment could then be calculated and compared with the total lipid mass determined by densitometry. The theoretical error in the percent interstitial lipid associated with these calculations was previously described as –27% and +10.5% (absolute errors typically of –1.13 and +0.44%). Because interstitial lipid is often referred to in terms of the percentage of muscle mass it occupies, the muscle mass of the slices was also determined. This was calculated by taking the total number of voxels in the ROI and subtracting the adipose voxels. The remaining voxels were assumed to muscle. This muscle volume was then converted to a mass by assuming a constant density of 1.07 g/ml (Allen *et. al.*, 1959). The lipid mass could then be expressed as a percentage of the muscle in that segment.

Comprehensive procedures for data analysis can be found in appendix E.

Figure 3.1 is an example of a forearm end-analysis image after thresholding.

Figure 3.1: A forearm image after the threshold has been applied, indicating the white pixels as lipid and the black as water (muscle; non-lipid). 'A' is actually a transparent region where the radius has been eliminated from analysis; 'B' corresponds to the ulna.

3.4.3 Reliability Analysis

With such a complex analysis, it was important to ensure that the data and results were consistent and could be reproduced. Without reliability, the results could not be readily accepted and the methodology and analysis would have to be questioned.

To test the reliability of the analysis, three raw data files corresponding to each limb segment were selected at random and re-analyzed. This was performed to determine how reliable the selection of the ROI is using the same protocol and software. Therefore, the same computer and software were used.

3.4.4 Statistical Analysis

The study was a block design, with all subjects receiving all interventions and the MRI scans performed at all twelve sites. Because the data of the three slices from each segment were collected simultaneously, the values are not independent and must be combined to perform statistical analysis on them.

Descriptive statistics were performed for the interstitial lipid of the limb segments and a combined average and variability was determined for all interstitial lipid values for each subject. Analysis of the data was performed to assess intra and intersegmental variability. As a secondary analysis, specific comparisons between the upper arm vs. forearm (UA vs. FA), upper leg vs.

lower leg (UL vs. LL), and upper arm vs. lower leg (UA vs. LL) were also assessed. These comparisons were performed based on the segments being part of the same limb (UA vs. FA; UL vs. LL) and similar size (UA vs. LL). Correlations between interstitial lipid and total body fat were calculated.

The power of the study was calculated in advance using the interstitial lipid chemical-extraction data of Hudson (1996).

$$\frac{n \sum_{i=1}^{4} (x_i - \bar{x})^2}{4\sqrt{18.24}} = \phi^2$$

n (0.2626) = ϕ^2; using the sample size (n) of 20 produced:

20 (0.2626) = ϕ^2; therefore:

$\phi = 2.3$; a-1 = 3; n-1 = 19. These values produced a power of 0.98.

Statistical analysis was performed using two computer programs: Stataquest 3.1 (Stata Corp., College Station, TX) and Minitab 8.1 (Minitab Inc., State College, PA) on a Power Macintosh (Apple Computer, CA).

CHAPTER 4

RESULTS & ANALYSIS

PART I - RESULTS

This chapter presents the anthropometric, underwater weighing, and magnetic resonance imaging data for all twenty subjects, including the statistical analysis of the data. Equations for calculations of total body fat, anthropometric muscle mass and conversion formulas for the MRI results can be found in appendices F and G. The screening anthropometric body fat data is listed in appendix H.

4.1 Densitometry Results

Underwater weighing and residual volume values were obtained from all twenty subjects and a total body fat calculated using the formula from Siri (1956) (Table 4.1).

Subjects ranged in age from nineteen to twenty-eight years old. The subjects had backgrounds with a wide range of physical activity; some exercised for several hours per day whereas others exercised for a few hours every month. Their total body fat ranged from between five to thirty-six percent by mass. The mean (SE) body fat of all subjects was 16.54 (8.9)%. This falls within normal parameters for a healthy, young, male population

(Malina *et. al.*, 1991). The residual lung volumes also fall within the range expressed by Wilmore *et. al.* (1980).

Table 4.1: Data from underwater weighing, residual volume and percent fat values.

Subject	Age	Ht (cm)	Wt (kg)	Underwater Weight (kg)	Residual Volume (L)	Dens. (g/ml)	% Fat Siri*
1	22	175	114.9	1.4	0.91	1.017	36.86
2	23	183.1	69.4	3.7	0.98	1.070	12.60
3	27	184.8	83.85	4.3	1.4	1.070	12.60
4	20	179.4	81.5	4.7	1.5	1.079	8.76
5	22	181.0	89.1	5.3	1.225	1.075	10.51
6	21	188.6	87.2	5.01	1.435	1.077	9.61
7	23	187.1	75.0	3.3	1.440	1.065	14.79
8	22	167.8	84.15	1.03	1.202	1.023	33.87
9	25	195.5	90.6	4.6	1.546	1.069	13.05
10	27	186.7	85.3	4.05	1.575	1.066	13.96
11	23	177.5	78.2	4.053	1.161	1.068	13.65
12	23	190.9	92.8	5.00	1.484	1.072	11.96
13	25	169.5	71.8	2.70	1.11	1.053	20.08
14	22	187.6	99.5	4.00	1.510	1.054	19.37
15	23	173.1	59.7	2.7	1.351	1.069	12.96
16	23	181.9	68.6	4.1	1.574	1.087	5.26
17	26	173.35	70.05	4.41	1.021	1.081	7.95
18	28	170	83.55	1.14	1.539	1.027	31.98
19	19	182.9	81.15	4.17	0.905	1.063	15.53
20	20	166.8	88.3	2.798	1.001	1.041	25.41
Mean	23	180.13	82.73	3.62	1.29	1.06	16.54

*Siri (1956).

4.2 Magnetic Resonance Imaging Results

Because of the volume of the MR slice data, it is summarized in appendix I. Descriptive statistics of the data will not be presented here; it will be presented in the following section with the statistical analysis because

arbitrarily combining the slice data would not be prudent until appropriate statistical analysis has been performed. A "dot plot" is presented in figure 4.1 to give a general indication of the interstitial lipid distribution prior to statistical analysis, with histograms of interstitial lipid distribution appearing in appendix J.

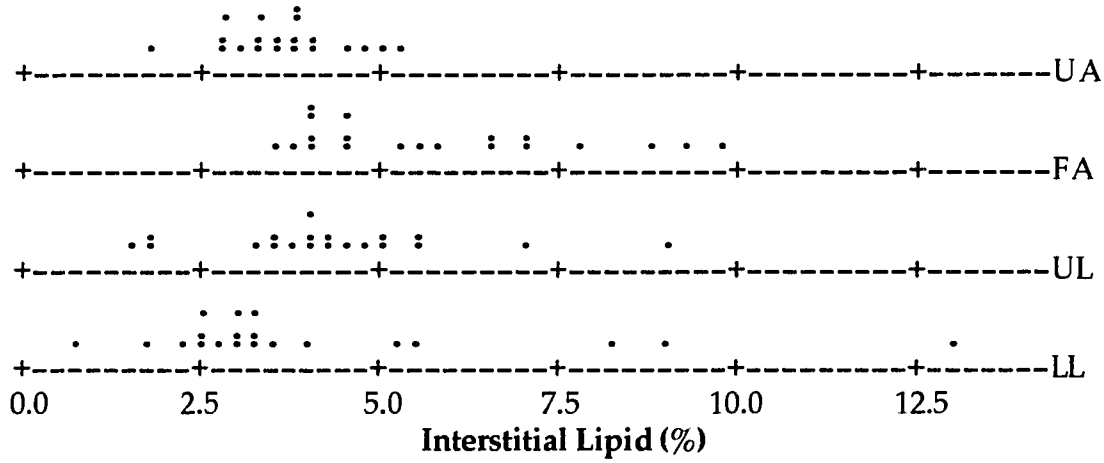

Figure 4.1: Dot plot indicating the distributions of interstitial lipid (%) for the four right-sided limb segments: upper arm (UA), forearm (FA), upper leg (UL), lower leg (LL).

The dot-plot in figure 4.1 indicates all of the limb segments do not have a bell-shaped normal distribution. The one lower leg value was re-appraised because it may be an outlier. Review of the analysis revealed that it is the correct value for that slice. The value belonged to an individual with high total body fat, as was desired so an accurate description of interstitial lipid's variability could be assessed. Therefore, it was not rejected.

4.3 Anthropometric Results

Anthropometric results are summarized in table 4.2.

Table 4.2: Girths and skinfold measurements were taken from each limb segment and detailed in Appendix G. Sites are from forearm (FA), upper arm (UA), upper leg (UL), and lower leg (LL). The skeletal muscle mass (kg M) and percentage (% M) are calculated according to Martin *et. al.* (1990).

	Girths (cm)				Skinfolds (mm)				Wt (kg)	Ht cm	kg M	% M
	FA	UA	UL	LL	FA	UA	UL	LL				
1	31.9	42.0	66.5	46.0	9.8	6.6	13.2	14.6	114.9	175	62	55
2	26.3	27.5	52.1	35.4	5.2	3.2	10.8	10.4	69.4	183	40	58
3	30.3	34.2	57.2	36.3	4.8	4.6	9.0	7.6	83.8	185	51	61
4	30.8	34.5	58.9	36.2	5.6	3.8	12.4	6.8	81.5	179	51	63
5	29.1	35.1	62.7	41.7	6.0	4.2	6.2	9.0	89.1	181	52	64
6	30.5	35.8	57.4	39.1	6.0	4.0	9.2	7.8	87.2	189	53	62
7	28.6	32.4	53.8	37.3	5.8	3.4	9.2	8.6	75.0	187	45	63
8	28.3	52.4	60.3	39.4	12.4	9.4	10.8	19.6	84.2	168	52	56
9	29.2	30.8	55.4	38.1	5.0	7.0	11.2	6.9	88.9	196	53	58
10	28.8	29.7	60.1	40.2	5.5	4.7	10.6	4.8	85.3	188	56	66
11	28.3	33.1	57.6	38.9	6.2	4.2	16.2	10.0	78.2	178	43	59
12	31.4	35.1	58.9	39.9	5.2	4.2	13.4	5.7	92.8	191	57	61
13	28.2	30.2	53.8	37.6	5.4	3.1	8.6	9.9	71.8	169	42	59
14	31.8	37.9	63.7	41.3	6.8	4.4	19.7	9.4	100	188	60	60
15	25.7	27.5	49.8	33.5	4.2	3.6	8.2	5.3	60	175	36	60
16	27.7	31.0	50.9	35.1	3.7	2.9	5.1	4.1	69	182	43	62
17	27.5	31.4	54.5	34.9	3.2	3.4	5.4	3.7	70	173	41	62
18	28.1	34.5	54.3	36.5	13.4	5.2	16.7	14.4	84	170	39	47
19	27.8	29.4	55.9	37.2	6.6	5.8	13.2	14.0	81	183	45	56
20	30.2	36.7	62.7	40.5	8.2	5.6	23.4	18.8	88.3	167	47	54
Mean	29.0	34.0	57.3	38.3	6.4	4.7	11.6	9.6	82.7	180	51	57

PART II - STATISTICAL ANALYSIS

4.5 Statistical Results

The design of the study has each subject providing data from all slices, therefore data was termed to be "blocked". Block design, or paired data, is not independent and requires specific statistical methods for correct analysis.

Clarification should be provided regarding the hypotheses for the following statistical tests. It was previously hypothesized that the interstitial lipid should have little intersegmental variability; this though was not the alternative hypothesis for the statistical analyses. The statistical tests are designed with the alternative or research hypothesis (H_A or H_1) to be that there was a difference in interstitial lipid between sites. The null hypothesis (H_0) therefore was that there was not a difference in interstitial lipid between sites. Therefore, if the p-value is greater than 0.05, the null hypothesis would be accepted as no difference in interstitial lipid between sites. If the p-value is less than or equal to 0.05, the null hypothesis was rejected, indicating that the interstitial lipid was different between sites.

The initial step in analysis of slice variability was to determine if the interstitial lipid of all slices were not statistically different. Because parametric tests are preferred, a blocked analysis of variance was considered. Unfortunately, the slice data did not conform to the assumption of equal variances for the residuals, and the residuals were not normally distributed, even when it was transformed using a natural log (ln) function, square root,

or inverse function. Therefore, a non-parametric Friedman test (Altman, 1991) was used to analyze the slices and determine if they could be combined (Table 4.3). The resulting p-value was <0.001; therefore the percent interstitial lipid for the twelve slices were considered statistically different and not combined.

Table 4.3: Friedman analysis comparing all slices. p-value <0.001.

Slice	N	Est. Median	Sum of Ranks
UA – 1	20	3.586	120.0
UA – 2	20	3.668	126.5
UA – 3	20	3.253	91.0
FA – 4	20	8.835	232.0
FA – 5	20	3.387	117.0
FA - 6	20	4.383	145.0
UL - 7	20	4.119	138.0
UL - 8	20	4.353	152.0
UL - 9	20	3.874	129.5
LL - 10	20	2.886	77.0
LL - 11	20	4.196	146.0
LL - 12	20	3.114	86.0

The power for the test was 0.97 based on an Analysis of Variance; therefore it will be slightly lower due to the non-parametric analysis.

The data is continuous, which fulfills the assumption for the Friedman analysis (Milton, 1992). Since the slices were not homogenous overall, the approach was taken to compare the slices within each limb segment to determine if a mean could be determined for each limb segment. Table 4.4 indicates the results of the intrasegmental Friedman analysis.

Table 4.4: Friedman analysis comparing the interstitial lipid of the three slices within each limb segment. Ranks were given according to slice position.

Slice:	Forearm	Upper Arm	Upper Leg	Calf
P value:	<0.001	0.158	0.117	<0.001
Sum of Ranks:	60	43	39	32
	27	44	47	55
	33	33	34	33

The analysis indicated that the three slices from the upper arm were not statistically different and nor were the thigh slices at the 5% level of significance. The sum of ranks for the forearm indicated the proximal slice could not be combined with the other two; the same was true for the middle calf slice. Therefore, there was an indication of some inhomogeneity within two of the four segments.

Though the slices are statistically different, it merely indicated that the interstitial lipid was not homogenous throughout the limb segments, similar to measuring subcutaneous adipose at different sites. A mean percent interstitial lipid for each limb segment was desired to provide more concise comparisons with total body fat. Proper analysis would dictate that any intrasegmental slices rejected by statistical analysis not be included in a calculated mean. This though would not provide an accurate value because it would not provide an indication of the variability with the limb segment. Therefore, to provide a representative value for each limb segment, means are presented for each limb segment in table 4.6; the limb slices which are statistically different are not removed from these mean values.

An overall mean interstitial lipid for each subject was also calculated, with all slices included in the calculation. From a practical standpoint this was appropriate. The interstitial lipid from the various slices provided an indication of the variability of the interstitial lipid, but eliminating any aberrant slices from a mean calculation would provide an inaccurate display. The overall mean should provide a better general value for each subject's interstitial lipid because individuals may deposit interstitial lipid in different proportions at different sites. Therefore, an overall mean would account for these differences and provide a balanced interstitial lipid value in table 4.6.

A secondary analysis was performed to determine if there were differences between the mean interstitial lipid of specific segments (UA vs. FA; UL vs. LL; UA vs. LL). Altman (1991) explains that a non-parametric analysis of two groups is performed preferentially with a Wilcoxan matched pair test over a Friedman analysis. Unfortunately, the Wilcoxan matched pair test is based on the assumption that the groups come from a population with a symmetric distribution; this assumption was not true for this data. Therefore, the Friedman analysis was performed to compare the specific segments. Table 4.5 demonstrates the result of this analysis.

Table 4.5: Friedman analysis comparing the interstitial lipid intersegmentally at the 5% level of significance.

Comparison:	All segments	UA vs. FA	UL vs. LL	UA vs. LL
p-value:	0.005	0.026	0.026	0.026

This analysis provided evidence that the limb segments, even under breakdown analysis, could not be considered similar in composition.

Table 4.6: Mean interstitial lipid MR data for each right-sided limb segment of all subjects. Limb segment data is expressed as the percentage of the regional muscle mass.

Subject	Total Body Fat %	FA %	UA %	UL %	LL %	Average IL%
1	36.86	9.04	3.75	9.04	12.93	8.69
2	12.60	9.57	3.56	4.51	3.03	5.19
3	12.60	7.15	2.91	5.59	2.78	4.61
4	8.76	4.30	2.76	4.09	1.76	3.23
5	10.51	4.63	3.25	3.62	3.31	3.70
6	9.61	4.15	2.64	3.24	2.89	3.23
7	14.79	5.40	3.36	5.06	2.37	4.05
8	33.87	10.02	4.15	7.01	9.01	7.50
9	13.05	6.75	2.71	5.11	5.46	5.01
10	13.96	5.99	4.72	5.59	3.30	4.90
11	13.65	3.63	5.28	4.11	5.16	4.55
12	11.96	5.81	3.42	4.25	2.39	3.97
13	20.08	4.00	4.93	4.64	3.17	4.19
14	19.37	4.68	4.09	4.33	4.09	4.30
15	12.96	4.66	3.29	3.77	3.42	3.79
16	5.26	4.29	1.80	1.68	0.72	2.12
17	7.95	4.21	3.77	1.50	2.62	3.02
18	31.98	7.15	3.83	3.41	8.30	5.68
19	15.53	6.78	4.49	1.74	2.97	3.99
20	25.41	7.90	3.53	3.93	2.56	4.49
Mean (SE)	16.54 (1.98)	6.01(0.44)	3.61(0.19)	4.31(0.39)	4.11(0.65)	4.51(0.33)

4.5.1 Reliability Results

Three slices were chosen at random from each limb segment to be re-analyzed for reliability testing. The slices were taken from their original raw

data state and transformed through the analysis algorithm to arrive at a percent interstitial lipid. Results are presented in Table 4.7.

The algorithms from the various computer programs should not effect the re-analysis, but because the region-of-interest is somewhat subjective, it was probably the most variable factor in the analysis.

Table 4.7: Data from the reliability tests indicating the percent interstitial lipid of the original scan and the subsequent re-analyzed scans. Scans are designated according to segment and slice (0,1, or 2).

Subject	Scan	%Lipid*	%Lipid**	Absolute Difference
3	LL-2	2.92	2.93	0.01
11	LL-1	3.38	3.64	0.26
16	LL-2	0.50	0.55	0.05
5	FA-1	4.00	4.07	0.07
6	FA-2	5.03	5.24	0.21
19	FA-1	2.08	1.96	0.12
1	UA-1	3.86	3.53	0.33
2	UA-1	5.50	5.66	0.16
13	UA-0	6.63	6.27	0.36
10	UL-0	5.60	5.44	0.16
14	UL-0	3.40	3.79	0.39
18	UL-0	4.33	4.38	0.05

***First analysis. **Second analysis.**

The best analysis for the reliability data was a blocked parametric analysis; each slice contributes both values. Table 4.8 displays the analysis.

Table 4.8: Blocked analysis of variance for the reliability data.

Source	df	Sum of Squares	Mean Sum of Squares	F	p-value
Subject	11	59.6756	5.4251		
Slices	1	0.0044	0.0044	0.17	0.6880
Within Error	11	0.2844	0.0258		
Total	23	59.9646	5.4553		

The resultant p-value indicated that both sets of reliability slice data was not statistically different at the 5% level of significance. The assumption of a normal distribution for the reliability analysis was satisfied in figure 4.2, with the equality of variances assumption also being satisfied. Variances for the two groups of data were 2.79 for the first set and 2.66 for the second set.

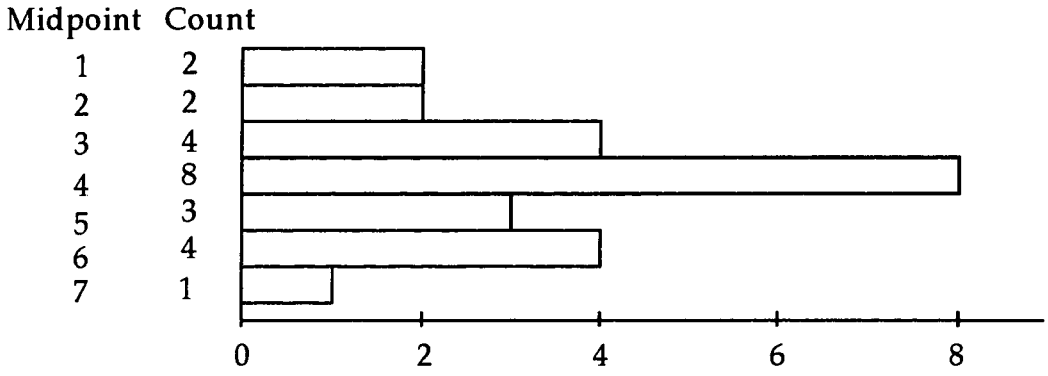

Figure 4.2: Histogram representing the distribution of the interstitial lipid values in the reliability analysis. General indication is symmetrical.

4.5.2 Interstitial lipid vs. Total body fat & Muscle Mass

It was hypothesized that the interstitial lipid would vary directly with total body fat. To test this hypothesis, correlation coefficients and corresponding p-values were calculated for mean interstitial lipid from each limb segment and the mean total interstitial lipid for each subject, against total body fat (Table 4.9).

Table 4.9: Correlation coefficients of the mean limb segment interstitial lipid (%IL) and the mean %IL of each subject with total body fat (%).

Segment:	UA	FA	UL	LL	Mean
Correlation Coefficient (r):	0.368	0.652	0.629	0.849	0.866
p-value:	0.103	<0.01	<0.01	<0.01	<0.01

Except for the correlation of the upper arm mean interstitial lipid with total body fat, which was not significant at the 5% level of significance, the interstitial lipid positively correlated with total body fat in the other segments with statistical significance. Graphical representation of the correlations were demonstrated in Figures 4.3, 4.4, 4.5, 4.6, 4.7, 4.8.

Correlation coefficients testing the relationship between mean total and segmental interstitial lipid with anthropometrically-determined percent muscle mass were determined (Table 4.10).

Table 4.10: Correlation coefficients of mean total and limb segment interstitial lipid (%) with skeletal muscle mass (%).

Segment:	UA	FA	UL	LL	Mean
Correlation Coefficient (r):	-0.236	-0.553	-0.149	-0.610	-0.557
p-value:	>0.20	<0.05	>0.20	<0.01	<0.01

The significant negative correlation of the forearm and calf with percent skeletal muscle mass suggested that there was some evidence that interstitial lipid decreased with an increase in proportionate skeletal muscle mass. Though the upper arm and upper leg were not significant at the 5% level of significance, overall evidence, including the significant negative

correlation between mean percent interstitial lipid and percent muscle mass, was indicative of a significant negative correlation. The relationship between the segmental and mean interstitial lipid for each subject was demonstrated graphically in figures 4.9, 4.10, 4.11, 4.12, 4.13.

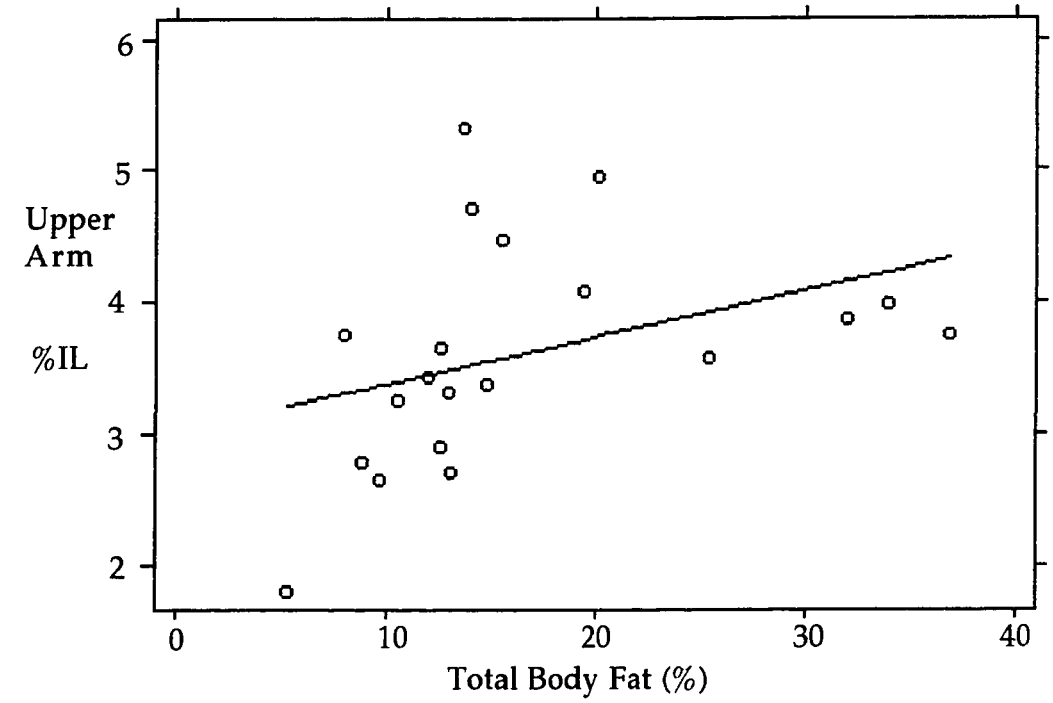

Figure 4.3: Correlation of mean upper arm percent interstitial lipid with total body fat (%).

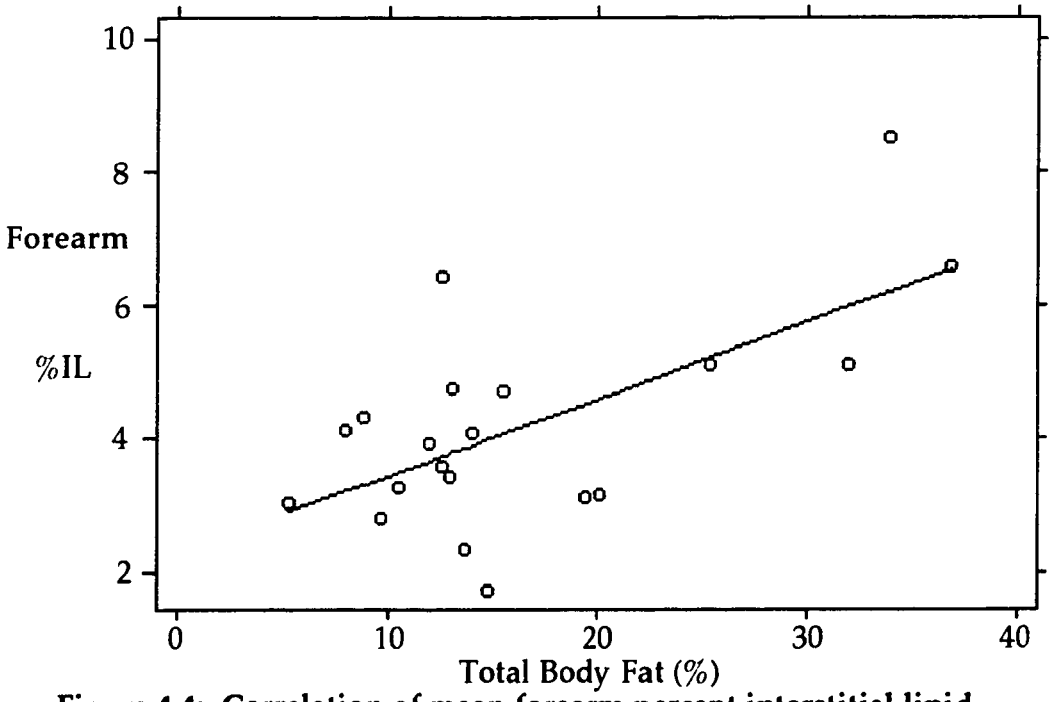

Figure 4.4: Correlation of mean forearm percent interstitial lipid with total body fat (%).

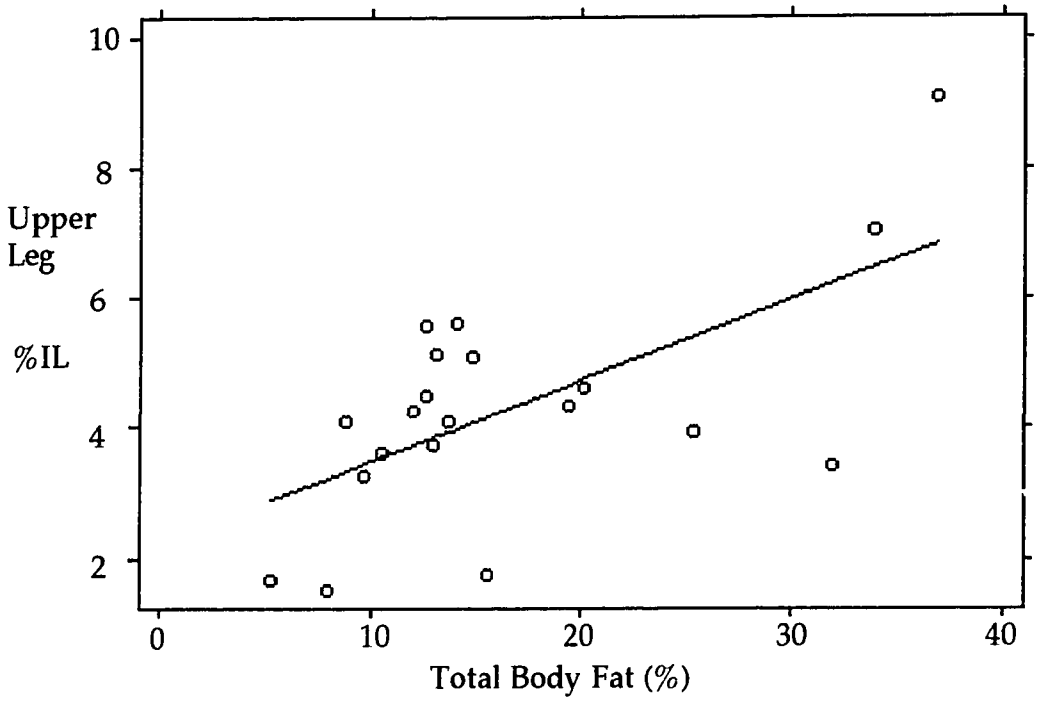

Figure 4.5: Correlation of mean upper leg percent interstitial lipid with total body fat (%).

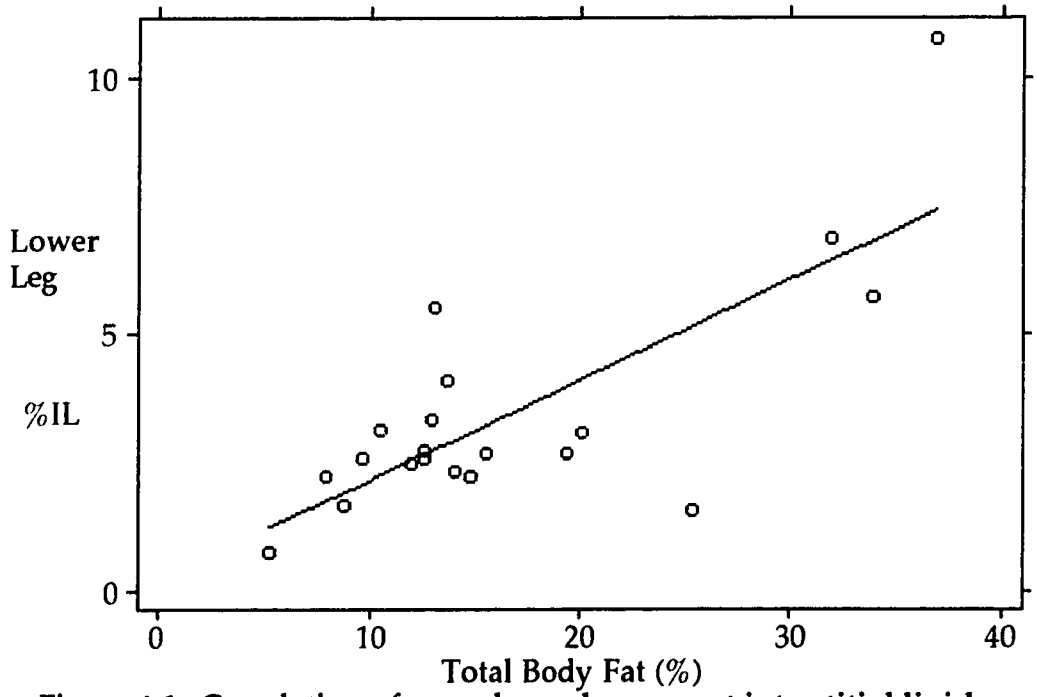

Figure 4.6: Correlation of mean lower leg percent interstitial lipid with total body fat (%).

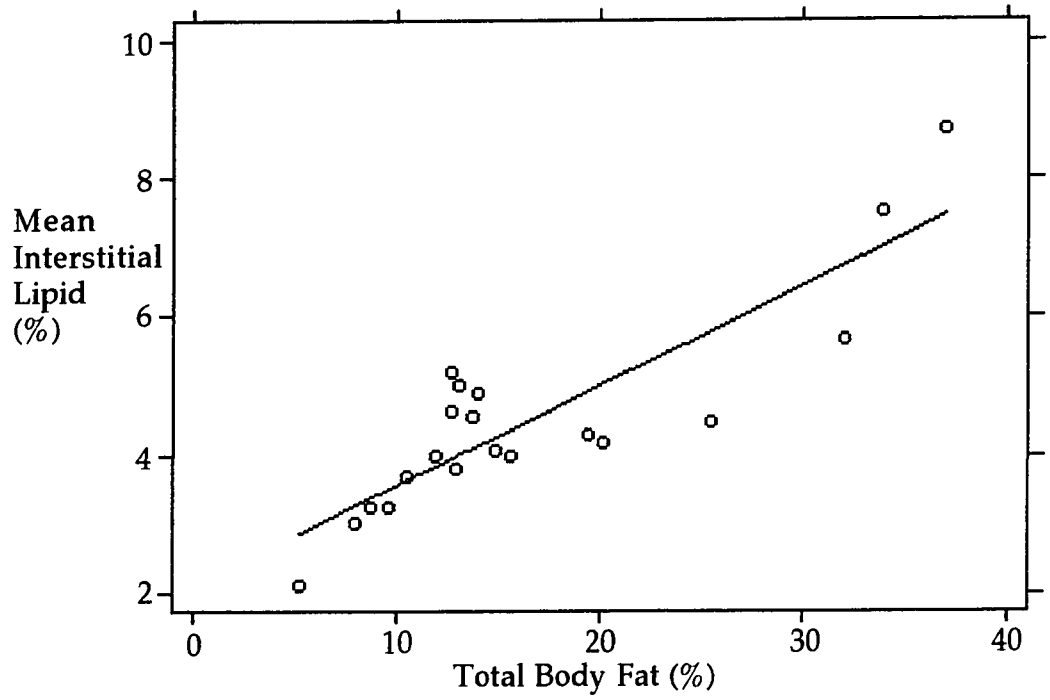

Figure 4.7: Correlation of mean interstitial lipid (%) for each subject with total body fat (%).

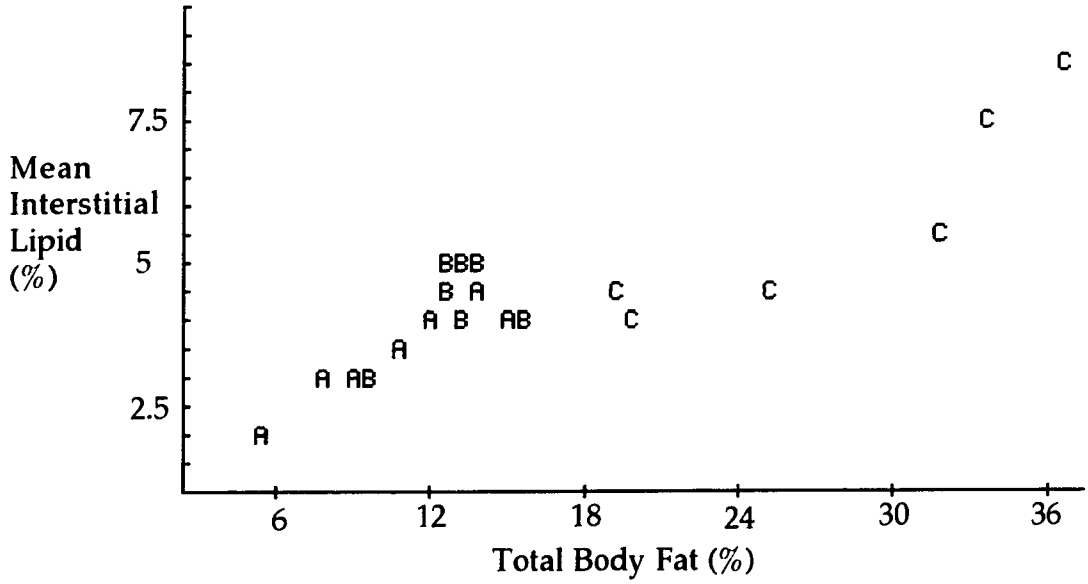

Figure 4.8: Mean interstital lipid (%) of each subject relating to total body fat (%). The initial screening data stratified the subjects into 3 groups according to percent body fat: A = <13%; B = 13-17%; C = >17%.

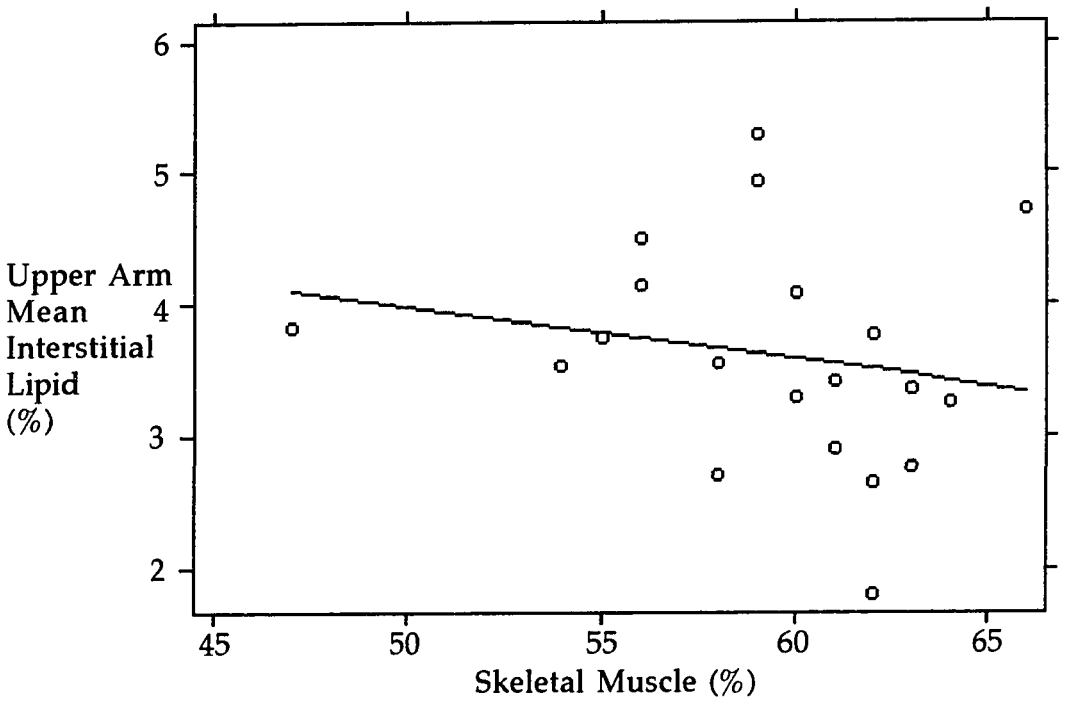

Figure 4.9: Relationship of the mean upper arm interstitial lipid (%) and proportionate skeletal muscle mass.

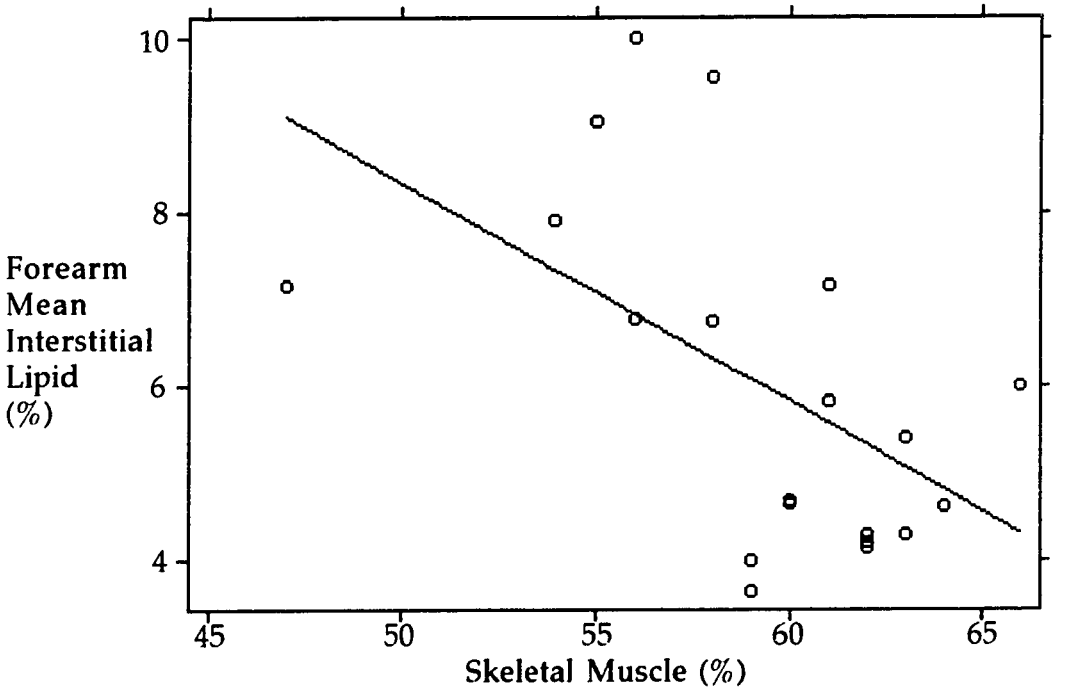

Figure 4.10: Relationship of the mean forearm interstitial lipid (%) and proportionate skeletal muscle mass.

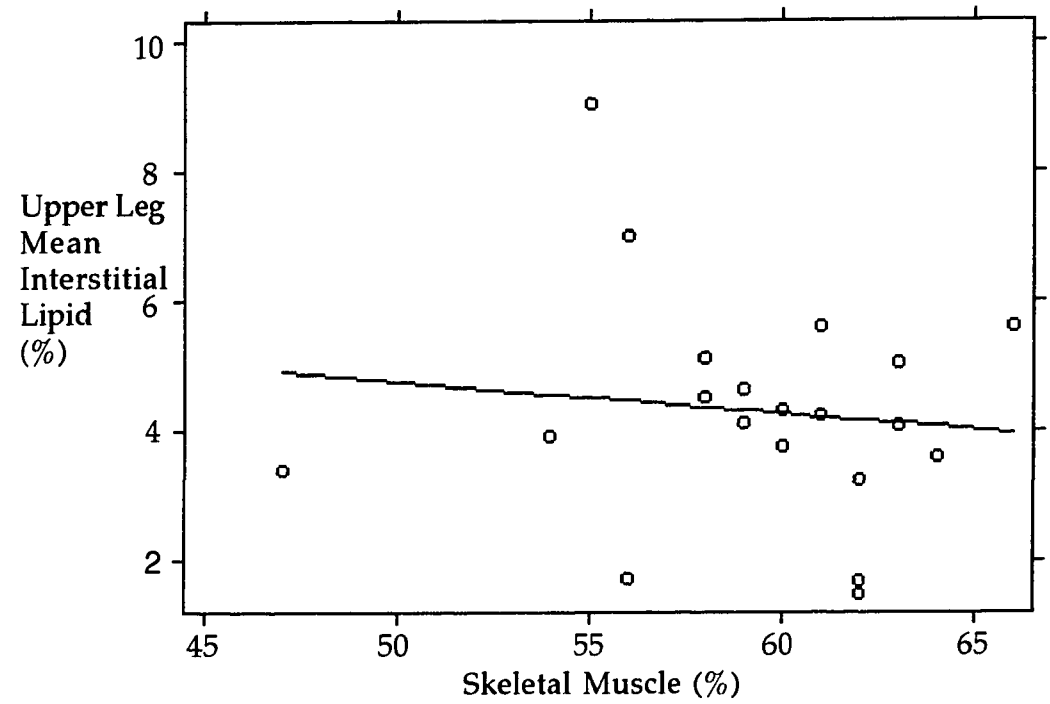

Figure 4.11: Relationship of the mean upper leg interstitial lipid (%) and proportionate skeletal muscle mass.

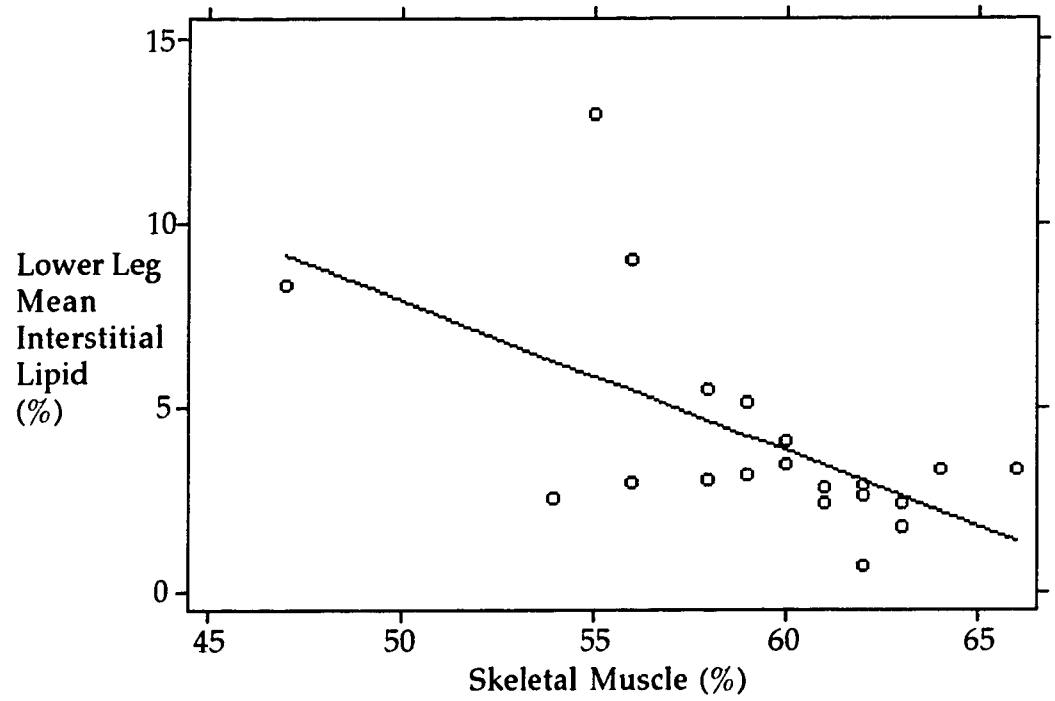

Figure 4.12: Relationship of the mean lower leg interstitial lipid (%) and proportionate skeletal muscle mass.

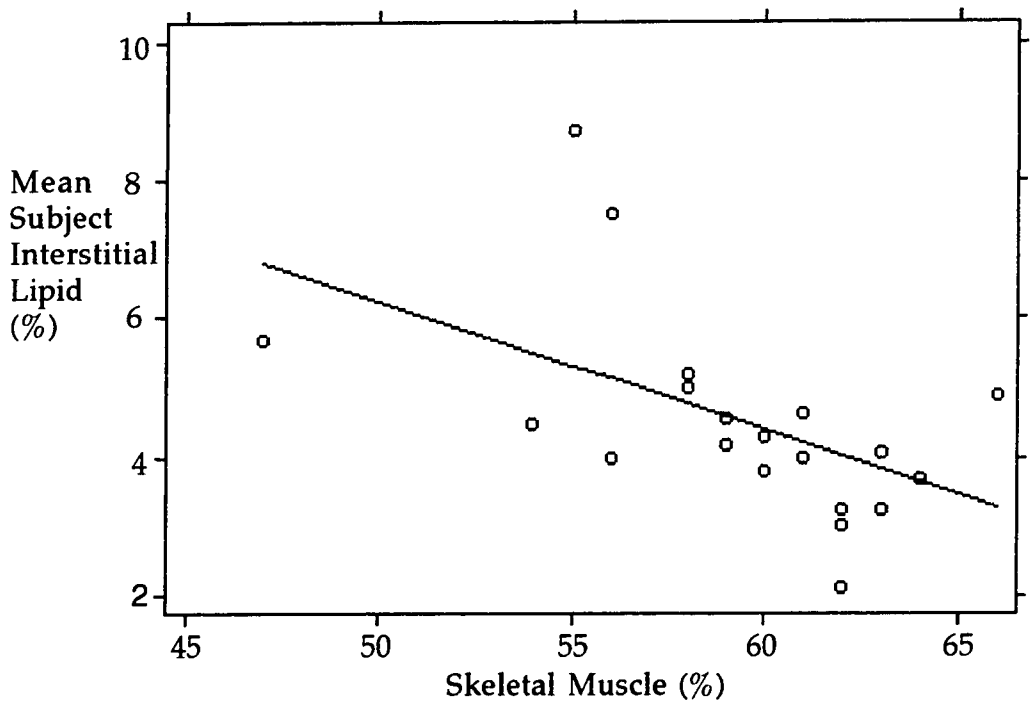

Figure 4.13: Relationship of the mean subject interstitial lipid (%) and proportionate skeletal muscle mass.

CHAPTER 5

DISCUSSION

5.1 Quantifying Interstitial Lipid with MRI

Interstitial lipid was quantified at selected sites *in vivo* using the magnetic resonance image-segmentation method. The values obtained for interstitial lipid range from 0.72 - 12.36%, with an average of 4.51%. These values are consistent with those reported in the literature for the cadaveric specimens of Mitchell *et. al.* (1945) and Forbes *et. al.* (1953), Forbes *et. al.* (1956), and Moore *et. al.* (1968), see Table 5.1.

Table 5.1: Comparison of interstitial lipid (IL) and total body fat (TBF %) data from various researchers. The "Current Study" has taken the mean value of overall interstitial lipid, total body fat, and age from the results; the other studies provide data from only one cadaveric subject each.

Study:	Mitchell *et. al.* (1945)*	Forbes *et. al.* (1953)*	Forbes *et. al.* (1956)*	Forbes *et. al.* (1956)**	Moore *et. al.* (1968)*†	Current Study*
IL (%):	3.35	6.60	9.40	2.22	2.9	4.51
TBF (%):	12.51	19.44	27.93	4.32	16.2	16.54
Age:	35	46	60	48	67	23^

* Caucasian **African-American † female ^average from twenty subjects.

5.2 Comparison of Interstitial Lipid with Total Body Fat & Muscle Mass

Because the subjects were representative of young, healthy males, the correlations of total body fat with interstitial lipid can be generalized for similarly aged males. The correlation coefficients for the mean of the three slices taken from the forearm, thigh, and calf percent interstitial lipid with percent total body fat were significant at 0.652, 0.629, and 0.849, respectively.

Only the interstitial lipid of the upper arm was not significantly correlated to total body fat (0.368). The upper arm vs. total body fat value is positive though with figure 4.4 demonstrating a positive trend. The lower correlation coefficient may be an indication that as total body fat increases, the upper arm accumulates less lipid with respect to the other sites. The correlation coefficient for the mean percent interstitial lipid for all twelve measurements of a subject and total body fat was 0.866 ($p<0.01$). The strong correlation in overall mean in comparison to individual segments may appear unusual, but may be possible. The overall mean takes into account all segments, balancing the values and indicating that overall, the individuals with higher body fat have more interstitial lipid than those with lower body fat. These values, in conjunction with figures 4.3-4.8, suggest that there is a direct relationship between interstitial lipid and total body fat.

These results were expected. As a person accumulates more lipid, it must be deposited in the lipid depots. Even if one depot accumulates the lipid preferentially, such as the lower leg, there is probably going to be some increase in the other depots, though perhaps not to the same extent, like in the upper arm.

The results from the correlation of interstitial lipid with proportionate skeletal muscle mass indicated the opposite trend. The interstitial lipid of the forearm and calf negatively correlated with skeletal muscle mass (-0.553 and –0.610, respectively), which were statistically significant ($p<0.05$, $p<0.01$,

respectively). The thigh and upper arm interstitial lipid values had no statistically significant correlation with skeletal muscle mass ($p>0.05$), though both values were also negative (-0.236, -0.149). Interpreting these results is difficult because it is assessing the relationship between regional interstitial lipid and total proportionate skeletal muscle mass and significant p-values simply indicate that the correlation coefficient is not zero. Figures 4.9-4.12 were very scattered; even though the correlation coefficients and regression lines were negative, the relationship between the mean limb segment interstitial lipid and proportionate skeletal muscle mass was not readily apparent. There was a negative relationship between the mean percent interstitial lipid and proportionate increases in muscle mass (-0.557, $p<0.01$), with the data in figure 4.13 having a much cleaner regression line with less scatter in the values than the limb segment values. This may be a better overall indicator of changes between interstitial lipid and proportionate skeletal muscle because this correlation is from a global interstitial lipid value, not specific to limb segments.

5.3 Intra & Intersegmental Variability

It was hypothesized that the interstitial lipid would not vary intrasegmentally. The results are somewhat supportive of this hypothesis. The upper arm slices were not statistically different from one another and the thigh slices were also not statistically different. The proximal forearm slice

and the middle calf slice were rejected from their respective segments; both of these slices had interstitial lipid values that were considerably higher than their counterparts. The following is an hypothesis for the elevated lipid in the forearm slice.

The proximal scan was taken at the level of the radial-ulnar articulation where the joint capsule was prominent. This scan had less muscle than the other two but had a high concentration of "residual" interstitial lipid because of the articulation. This residual lipid drastically increased the mean and variance of the forearm values. The definition of interstitial lipid included lipid associated with the muscle tissue and "residual lipid" that belongs in none of the other depots. Therefore, perhaps the interstitial lipid within the muscle tissue has a differing pattern and percentage than the "residual" lipid, as evidenced in Table 5.2.

A simple anatomical reason does not exist for the difference in the middle calf slice. Perhaps the greater interstitial lipid content in the calf at the maximum girth is for support due to the constant weight-bearing of the lower leg. The MRI slices were sampling the interstitial lipid from continuous sections of tissue, which were not necessarily homogenous from one end of the limb segment to the other.

Table 5.2: Interstitial lipid: intramuscular vs. residual. The values for "skin, muscle and residual" refer to the lipid within those tissues. All values are in kg. Each study listed is data from one cadaveric subject.

Tissue	Mitchell *et. al.* (1945)*	Forbes *et. al.* (1953)*	Forbes *et. al.* (1956)*	Forbes *et. al.* (1956)**	Moore *et. al.* (1968)†
Adipose	4.08	4.38	12.48	0.14	1.20
Non-adipose lipid	4.75	6.08	8.05	2.54	2.61
Skin	0.72	0.49	0.94	0.28	0.41
Muscle	0.75	1.41	2.78	0.59	0.30
Residual	1.48	1.81	1.91	0.63	1.84
Total Fat (kg)	8.83	10.46	20.53	2.68	3.81

* Caucasian **African-American † female.

Similar patterns are true of subcutaneous adipose tissue. If cross-sections of the abdomen or trunk are considered, subcutaneous adipose forms a continuous layer in the area, but the patterning changes if a more superior or inferior site is chosen. Though interstitial lipid is fairly homogenous within a limb segment, differences may be noted depending on the site chosen.

Intersegmental variability for interstitial lipid indicated that limb segments were statistically different, even though the lipid within a limb segment was fairly constant. These results suggest that the human body deposits of interstitial lipid may not differ much locally but rather, having differing global patterns throughout the body, similar to subcutaneous patterning.

The mean interstitial lipid of the forearm slices has the highest values. This could be due to the vast number of individual muscles in the forearm. Between each muscle belly, adipose tissue serves as cushion and protector. Therefore, the forearm would have a higher percentage of interstitial lipid. Though the other three limb segments have similar mean interstitial lipid values, with the upper leg having the highest mean (4.31), the lower leg having a mean of 4.11, and the upper arm having the lowest mean percent interstitial lipid (3.61). The upper leg has several muscle bellies within a cross-sectional image as compared to the upper arm, perhaps contributing to the higher interstitial lipid component. The muscles in the upper leg are large, requiring the interstitial lipid for support and metabolic needs.

5.4 Densitometry Appraisal

The densitometry and residual volume procedures were successful with no subjects experiencing any adverse effects.

The mean (16.54%) and standard deviation (8.9%) of the total body fat were acceptable, being similar to male population values (Malina et. al, 1991). The standard deviation may be somewhat elevated but the extreme body fat values were desired for this study to achieve results from a broad cross-section of young, healthy males.

5.5 Magnetic Resonance Appraisal

The MR image segmentation method has been a common lipid/adipose analysis tool in the literature. Since this study was the first to employ this technique in this laboratory, it will be appraised focussing on the analysis and its generalizability.

Unfortunately, there are several factors which limits the creation of a standard protocol that can be used universally. Software is the most critical and most uncontrollable of these factors. The analysis protocol used in this study implemented a variety of programs, both in-house and commercial that fulfilled our needs. At another research facility different software packages may be present that could achieve the goal of quantifying lipid. The end result of quantification of lipid should be similar but the specifics of the software packages would limit the transferability of specific protocols between research institutes.

By focussing on the protocol used in this study, the specific portions that are not generalizable would be the contrast, brightness, region-of-interest, and thresholds. The contrast and brightness were adjusted to enhance the regions so the lipid could be better differentiated from the non-lipid tissues. Changing these values would not necessarily alter the end results, but a different threshold would have to be selected. Because the region-of-interest is somewhat subjective, reliability tests were performed and will be discussed subsequently. The threshold is also somewhat of a subjective value. This is

mainly due to the fact that the magnetic field within the scanned tissue is not necessarily homogenous within a scanned area, let alone between two different scans using the same pulse sequence. For this reason, a general value for the threshold was set at 195 but was altered slightly to accommodate images where the pixel intensity of lipid regions was altered due to "ghosting". This is why the contrast and brightness were kept constant, so a general standard could be used as a comparison.

The assessment of reliability by re-analyzing some random scans using Photoshop were assuring. The absolute values differed from one another from between 0.01-0.39% interstitial lipid. These results suggest that using the same protocol, an experienced analyst can arrive at very reliable values.

5.6 Limitations

This study was not without limitations. Many assumptions with regards to calculations and methodology have been stated previously, but will be summarized here. Those include the inherent assumptions of densitometry, and those utilized in the conversion formulas for MR data.

The use of underwater weighing to arrive at a value for body density through Archimedes Principle of Water Displacement has been accepted without controversy in the scientific community. It is the assumptions made by densitometry in converting that density to a value of body fat which are controversial, introducing an error as high as 25% in fat estimation.

Obviously, all of the twenty subjects will not fulfill all of the densitometry assumptions perfectly, but all of the subjects are similar to those cadaveric specimens used to arrive at the densitometry equations. Therefore, though the values are not going to be perfect for each individual, the resultant total body fat values cannot be any more accurate with present technology and resources.

This also holds true for the assumptions used in the MR analysis. Assumptions regarding adipose tissue composition and density were made to arrive at usable interstitial lipid values. The subjects will have some variability around the assumed "constant" values, but since the subjects are healthy individuals, the variance should not be extreme. If the lipid fraction of the adipose tissue was similar to the extreme values of the literature, the interstitial lipid may be overestimated by a factor of 25% or underestimated by a factor of 10.5%.

The interstitial lipid was also assessed at only twelve sites on young males. The results should therefore be considered realizing that perhaps a greater or lesser variability in interstitial lipid exists globally within an individual. Because interstitial lipid was only assessed at twelve sites, no calculations were made with regard to predicting interstitial lipid from total body fat or skeletal muscle mass. Because of the differences in the human body between different ages and gender, the results should be considered within only the young, healthy, male population.

5.7 Conclusions & Future Considerations

The study achieved the following goals:

- Quantified interstitial lipid at specified sites *in vivo.*
- Compared the relationship of interstitial lipid with total body fat.
- Assessed interstitial lipid's variability within a limb segment and between limb segments.

The *a priori* hypotheses were also answered:

- Interstitial lipid did vary directly with total body fat.
- The hypothesis of a constant patterning for interstitial lipid throughout the body received little evidence; variability in its deposition was demonstrated.

The evidence against the second hypothesis can be supported. If subcutaneous adipose tissue is considered as a model, it has a variable distribution throughout the body with differences occurring with respect to gender and age. Therefore the variable patterning of interstitial lipid was not an absolute surprise. The definition of interstitial lipid for this study included the lipid surrounding the vessels and nerves within the fascial compartment. If this definition is changed to classify interstitial lipid as only that lipid within the muscle tissue, then perhaps the interstitial lipid will demonstrate less variability.

A potential future study could evaluate interstitial lipid within an individual and then re-evaluate that individual at a later time and possibly after some intervention, a marathon for example, to assess changes to interstitial lipid.

A future study may also evaluate interstitial lipid over a greater section of the body by taking more slices at greater intervals and interpolating between the slices to arrive at a better indication of the variability and overall value. This type of study, in conjunction with accurate total body fat and skeletal muscle mass assessments may provide a multivariate regression analysis to better predict interstitial lipid from total body fat or other variables.

This study can serve as a baseline reference for interstitial lipid in young, healthy, males. With the ever-evolving pulse sequences and techniques available in MRI, future studies may be able to perform more extensive scanning while reducing the time and complexities of analysis. Future studies may also be able to determine if these quantities and variances for interstitial lipid are similar to those of females or different age groups.

REFERENCES

Abate N, Burns D, Peshock RM, Garg A, Grundy SM. Estimation of adipose tissue mass by magnetic resonance imaging: validation against dissection in human cadavers. *Journal of Lipid Research.* 35: 1490-1496. 1994.

Allen TH, Krzywicki HJ, Roberts JE. Density, fat, water and solids in freshly isolated tissues. *Journal of Applied Physiology.* 14(6):1005-1008. 1959.

Altman DG. *Practical statistics for medical research.* London: Chapman & Hall. 1991.

Atkinson T, Fowler VR, Ganton GA, Lough AK. A rapid method for the accurate determination of lipid in animal tissues. *Analyst* 97:562-568. 1972.

Bakker HK, Struikenkamp RS. Biological Variability in lean body mass estimates. *Human Biology.* 49: 187-202. 1977.

Baumgartner RN, Rhyne RL, Troup C, Wayne S, Garry PJ. Appendicular skeletal muscle areas assessed by magnetic resonance imaging in older persons. *Journal of Gerontology.* 47;3:M67-72. 1992.

Bax A, Lerner L. Two-dimensional nuclear magnetic resonance spectroscopy. *Science.* 232:960-967. 1986.

Behnke AR, Feen BG, Welham WC. Specific gravity of healthy men. *Journal of American Medical Association.* 118:495-8. 1942.

Bloch I. Nuclear Induction. *Physics Review*. 70:46-474. 1946.

Bottomley PA, Foster TB, Darrow RD. Depth-resolved surface-coil spectroscopy (DRESS) for in vivo ^{1}H, ^{31}P, and ^{13}C NMR. *Journal of Magnetic Resonance*. 59:338-342. 1984.

Brateman L. Chemical shift imaging: a review. *American Journal of Roentgenology*. 146:971-980. 1986.

Brozek J, Grande F, Anderson JT, Keys, A. Densitometric analysis of body composition: revision of some quantitative assumptions. *Annuls of New York Academy of Science*. 110:113-40. 1963.

Bruhn H, Frahm J, Gyngell ML, Merboldt KD, Hanicke W, Sauter R. Localized proton NMR spectroscopy using stimulated echoes: applications to human skeletal muscle in vivo. *Magnetic Resonance in Medicine*. 17, 82-94. 1993.

Buxton RB, Wismer GL, Brady JT & Rosen BR. Quantitative proton chemical-shift imaging. *Magnetic Resonance in Medicine*. 3:881-890. 1986.

Chumlea WC, Roche AF, Mukherjee D. Some anthropometric indices of body composition for elderly adults. *Journal of Gerontology*. 41:36-9. 1986.

Clayman, CB, Medical Editor. *The American Medical Association Encyclopedia of Medicine*. Random House, New York. 1989.

Dixon WT. Simple proton spectroscopic imaging. *Radiology,* 153:189-194. 1984.

Ernst RR, Anderson WA. Application of Fourier transform spectroscopy to magnetic resonance. *Review of Scientific Instruments.* 37: 93-102. 1966.

Fessenden RJ, Fessenden JS. *Organic Chemistry.* 4th ed. Pacific Grove, California: Brooks / Cole Publishing Company. 1990.

Forbes RM, Cooper AR, Mitchell HH. The composition of the adult human body as determined by chemical analysis. *Journal of Biological Chemistry.* 203:359-366. 1953.

Forbes RM, Mitchell HH, Cooper AR. Further studies on the gross composition and mineral elements of the adult human body. *Journal of Biological Chemistry* 223:969-975. 1956.

Fowler PA, Knight CH, Cameron GG, Foster MA. Use of magnetic resonance imaging in the study of goat mammary glands in vivo. *Journal of Reproduction and Fertility.* 89:359-66. 1990.

Fowler PA, Fuller MF, Glasbey CA, Cameron GG, Foster MA. Validation of the in vivo measurement of adipose tissue by magnetic resonance imaging of lean and obese pigs. *American Journal of Clinical Nutrition.* 56:7-13. 1992.

Frahm J, Haase A, Hanicke W, Matthaei D, Bomsdorf H, Helzel T. Chemical shift selective MR imaging using whole-body magnet. *Radiology*. 156: 441-444. 1985.

Fuller NJ, Jebb SA, Laskey MA, Coward WA, Elia M. Four component model for the assessment of body composition in humans: comparison with alternative methods and evaluation of the density and hydration of fat-free mass. *Clinical Science*. 82:687-693. 1992.

Garlick PB, Maisey MN. Magnetic Resonance Spectroscopy. *British Journal of Hospital Medicine*. 47; 5:330-334. 1992.

Gerard EL, Snow RC, Kennedy DN, Frisch RE, Guimaraes AR, Barbieri RL, Sorensen AG, Egglin TK, Rosen BR. Overall body fat and regional body fat distribution in young women: Quantification with MR imaging. *American Journal of Roentgenography*. 157: 99-104. 1990.

Haase A, Frahm J, Hanicke W, Matthaei D. ^{1}H NMR chemical shift selective (CHESS) imaging. *Physics in Medicine and Biology*. 30: 341-344. 1985.

Hashemi RH, Bradley WG. *MRI the basics*. Williams & Wilkins, Baltimore. 1997.

Heiken JP, Lee JKT, Dixon WT. Fatty infiltration by proton spectroscopic imaging. *Radiology*. 157: 707-710. 1985.

Heyward VH. Evaluation of body composition. *Sports Medicine*. 22 (3): 146-156. 1996.

Horton HR, Moran LA, Ochs RS, Rawn JD, & Scrimgeour KG. *Principles of Biochemistry*. Englewood Cliffs, N.J.: Prentice Hall. pp. 9.1-9.36. 1993.

Hudson SB. Validation Of Chemical Shift Imaging Against Organic Solvent Lipid Extraction: Quantification Of Lipid In Cadaveric Skeletal Muscle. Masters Thesis. University of Calgary. 1996.

Iles RA, Griffiths JR, Stevens AN. NMR studies of metabolism in living tissues. *Progress in Nuclear Magnetic Resonance Spectroscopy*. 15:49-200. 1982.

Iles RA, Chalmers RA. Nuclear magnetic resonance spectroscopy in the study of inborn errors of metabolism. *Clinical Science*. 74:1-10. 1988.

Knight CH, Fowler PA, Wilde CJ. Galactopoietic and mammogenic effects of long-term treatment with bovine growth hormone and thrice daily milking in goats. *Journal of Endocrinology*. 127:129-38. 1990.

Kohrt WM. Body composition by DXA: tried and true? *Medicine and Science in Sports and Exercise*. 27;10:1349-1353. 1995.

Lee JKT, Dixon WT, Ling D, Levitt RG, Murphy WA. Fatty infiltration of the liver: Demonstration by proton spectroscopic imaging. *Radiology*. 153: 195-201. 1984.

Leroy-Willig A, Willig TN, Henry-Feugeas MC, Frouin V, Marinier E, Boulier A, Barzic F, Schouman-Claeys E, Syrota A. Body composition determined with MR in patients with Duchenne muscular dystrophy, spinal muscular atrophy, and normal subjects. *Magnetic Resonance Imaging*. 15; 7: 737-744. 1997.

Leusink JA. Fit, vet, vetvrije in vrije vetzuren. State University, Utrecht. 1972.

Lohman TG. Skinfolds and body density and their relation to body fatness: a review. *Human Biology*. 53:181-225. 1981.

Malina RM, Bouchard C. Growth, Maturation, and Physical Activity. Champaign, Illinois. Human Kinetics Publishers. 1991.

Martin AD, Ross WD, Drinkwater DT, Clarys JP. Prediction of body fat by skinfold caliper: assumptions and cadaver evidence. *International Journal of Obesity*. 9:1, 31-39. 1985.

Martin AD, Spenst LF, Drinkwater DT, Clarys JP. Anthropometric estimation of muscle mass in men. *Medicine and Science in Sports and Exercise*. Vol. 22, No. 5, pp. 729-733. 1990.

Martin AD, Drinkwater DT. Variability in the measures of body fat: Assumptions or technique? *Sports Medicine*. 11; 5:277-288. 1991.

Matiegka J. The testing of physical efficiency. *American Journal of Physical Anthropology*. 4: 223-230. 1921.

Matthaei D, Hasse A, Frahm J, Schuster R, Bomsdorf H. Chemical-shift-selective magnetic resonance imaging of avascular necrosis of the femoral head. *Lancet*. 1:370-371. 1985.

McElvoy AW, Jones OFW. Anthropometric indices in normal elderly subjects. *Age Aging*. 11:97-100. 1982.

McNeill G, Fowler PA, Maughan RJ, McGaw BA, Fuller MF, Gvozdanovic D, Gvozdanovic S. Body fat in lean and overweight women estimated by six methods. *British Journal of Nutrition*. 65:95-103. 1991.

Mendez J, Keys A. Density and composition of mammalian muscle. *Metabolism*, 9: 184-187. 1960.

Milton JS. *Statistical Methods in the Biological and Health Sciences*. 2nd ed. McGraw-Hill, Inc. 1992.

Mitchell HH, Hamilton TS, Steggerda FR, Bean HW. The chemical composition of the adult human body and its bearing on the biochemistry of growth. *Journal of Biological Chemistry*. 158:625-637. 1945.

Moore FD, Lister J, Boyden CM, Ball MR, Sullivan N. The skeleton as a feature of body composition. *Human Biology*. 40:136-188. 1968.

Narayana PA, Hazle JD, Jackson EF, Fotedar LK, Kulkarni MV. In vivo ^{1}H spectroscopic studies of human gastrocnemius muscle at 1.5 T. *Magnetic Resonance Imaging*. 6; 5:481-485. 1988.

Oldendorf W, Oldendorf W. *MRI Primer*. New York: Raven Press. 1991.

Parizkova J. Lean body mass and depot fat during ontogenesis in humans. In Nutrition, Physical Fitness and Health. In International Series on Sport Sciences, 7. J. Parizkova and V.A. Rogozkin, ed., (Baltimore: University Park Press). 24-51. 1978.

Pawan GES, Clode M. The gross chemical composition of subcutaneous adipose tissue in the mean and obese human subject. *Biochem. J.* 74, 9P. 1960.

Purcell EM, Torrey HC, Pound RV. Resonance absorption by nuclear magnetic moments in a solid. *Physics Review.* 69:37. 1946.

Pykett IL, Rosen BR. Nuclear magnetic resonance: *In vivo* proton chemical shift imaging. *Radiology.* 149: 197-201. 1984.

Radda GK. The use of NMR spectroscopy for the understanding of disease. *Science.* 233: 640-645. 1986.

Roberts N, Cruz-Orive M, Reid MK, Brodie DA, Bourne M, Edwards HT. Unbiased estimation of human body composition by the cavalieri method using magnetic resonance imaging. *Journal of Microscopy.* 171: 239-253. 1993.

Rosen BR, Wedeen VJ, Brady TJ. Selective saturation NMR imaging. *Journal of Computer-Assisted Tomography.* 8: 813-818. 1984.

Ross R, Leger L, Guardo R, de Guise J, Pis BG. Adipose tissue volume measured by magnetic resonance imaging and computerized tomography in rats. *Journal of Applied Physiology.* 70:2162-2172. 1991.

Ross R, Léger L, Morris D, de Guise J, Guardo R. Quantification of adipose tissue by MRI: relationship with anthropometric variables. *Journal of Applied Physiology*. 72 (2): 787-795. 1992.

Ross R, Shaw KD, Martel Y, de Guise J, Avruch L. Adipose tissue distribution measured by magnetic resonance imaging in obese women. *Journal of Clinical Nutrition*. 57: 470-475. 1993.

Schick F, Eismann B, Jung WI, Bongers H, Bunse M, Lutz O. Comparison of localized proton NMR signals of skeletal muscle and fat tissue *in vivo*: two lipid compartment in muscle tissue. *Magnetic Resonance in Medicine*. 29: 158-167. 1993.

Seidell JA, Bakker CJG, Van der Kooy K. Imaging technique for measuring adipose tissue distribution: a comparison between computer-assisted tomography and 1.5 T magnetic resonance imaging. *American Journal of Clinical Nutrition*. 51: 953-957. 1990.

Sepponen RE, Sipponen JT, Tanttu JI. A method for chemical shift imaging: demonstration of bone marrow involvement with proton chemical-shift imaging. *Journal of Computer Assisted Tomography*. 8: 585-587. 1984.

Siri WB. *The gross composition of the body*. In: Tobias CA, Lawrence J.H. eds. Advances in Biological and Medical Physics. Vol. 4. New York: Academic Press, 239-280. 1956.

Snyder WS, Cook MJ, Nasset ES, Karhausen LR, Howells GP, Tipton IH, eds. Report for the task group on reference man (ICRP report 23). Oxford, England: International Commission on Radiological Protection. 1984.

Staten MA, Totty WG, Kohrt WM. Measurement of fat distribution by magnetic resonance imaging. *Investigative Radiology.* 24:345-349. 1989.

Stryer L. *Biochemistry.* 3rd ed. New York: W. H. Freeman and Company. 1975.

Thomas LW. The chemical composition of adipose tissue of man and mice. *Quarterly Journal of Experimental Physiology.* 47, 179-188. 1962.

Wang Z, Pierson, RN Jr., Heymfield SB. The five-level model: a new approach to organizing body-composition research. *American Journal of Clinical Nutrition.* 56:19-28. 1992.

Widdowson EM, McCance RA, Spray CM. The chemical composition of the human body. *Clinical Science.* 10: 113-125. 1951.

Wilmore JH, Vodak PA, Parr RB, Girandola RN, Billing JE. Further simplification of a method for determination of residual lung volume. *Medicine and Science in Sports and Exercise,* 12: 216-218. 1980.

Wong W., Northrup RS, Herrick RC, Blombicki AP, Wood RP & Morrisett JD. Quantification of lipid in biological tissue by chemical-shift magnetic resonance imaging. *Magnetic Resonance in Medicine.* 32: 440-446. 1994.

COMPUTER PROGRAMS

Adobe Systems. © 1989-1998. *Photoshop*. Version 5.0

Crawley, A. © 1995. *rawnhtofold*.

Crawley, A. © 1997. *rawmssplit*.

Chow K, & Smith, M. © 1992, 1994. *Viewdiff*, Version 3.3.

McGibney G. 1992. *Phasefit*..

Minitab Inc. © 1991, 1993. *Minitab Statistical Software*. Version 8.2.1.

Stata Corporation. © 1993. *Stataquest*, Version 3.1.

Lemkesoft © 1998 *Graphic Converter*. Version 3.2.

Appendix A

Lipids

In biological tissues, lipids occur in many configurations including prostaglandins, and cholesterol. The following figures are examples of these lipid categories.

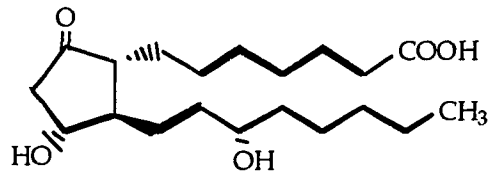

Figure 1: PGE_1 Prostaglandin

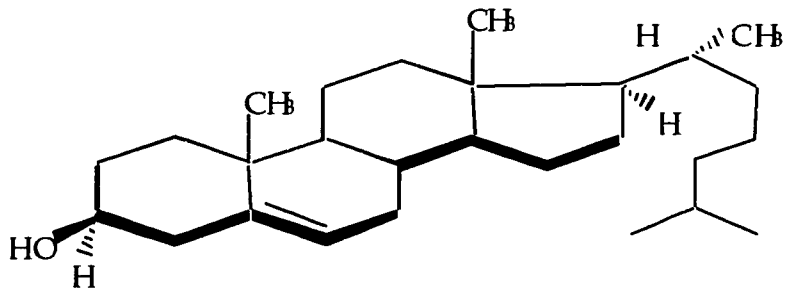

Figure 2: Cholesterol, a common steroid.

Appendix B

Exclusion Criteria

Subjects had to meet a variety of criteria based on both the MRI and densitometry methods. By combining the requirements of both methods, the following exclusion criteria was completed by all potential candidates:

Have you ever had a metallic foreign body in your eye?

Do you have:

- cardiac pacemaker, wires or defibrillator?
- artificial cardiac valve? If YES, what make and model?_____
- aneurysm clip?
- ear implant?
- eye implant?
- electrical stimulator for nerves and bones?
- other implanted device(s) or Metallic objects in body?
- Have you ever had surgery in your upper arm, forearm, thigh, or calf?
- Are you claustrophobic?
- Do you weigh over 260 lbs. (120 kg)? If YES, how much?_____

Are you able to climb a 7′ ladder and enter and exit a 2.5 m^3 tank without assistance?

Appendix C

Consent Form

Dr. Preston Wiley
Richard J. Schaan
Faculty of Kinesiology
Department of Sport Medicine
University of Calgary

Research Project Title: *Quantification of interstitial fat in vivo using* chemical shift imaging technique.
Investigators: Dr. Preston Wiley, Dr. Carla Wallace, Dr. Michael Hawes and Richard J. Schaan
Sponsor: Funding is provided by the Olympic Oval Fund at the University of Calgary.

This consent form, a copy of which has been given to you, is only part of the process of informed consent. It should give you the basic idea of what the research is about and what your participation will involve. If you would like more detail about something mentioned here, or information not included here, you should feel free to ask. Please take the time to read this carefully and to understand any accompanying information.

In this study, we are determining the amount of fat within muscle tissue (interstitial fat) using magnetic resonance imaging (MRI). This data will be compared to total body fat which will be determined using densitometry (underwater weighing) and an estimation of muscle mass. Muscle mass will be determined by taking skinfold measurements and girths.

Very little research has been performed on interstitial fat in the past so little is known about its amount or its distribution within the body. Most prior studies have used cadavers, not living people. This study will focus on interstitial fat in living human beings.

The MRI's will take approximately one hour. Twelve scans in total will be taken from your upper arm, forearm, upper leg, and lower leg on the right side of your body. MRI does not expose you to any radiation and has no known side effects.

Densitometry measures total body fat by converting your body density which is determined by underwater weighing. You will submerse in a tank of water (approximately 2 cubic meters) and release the air in your lungs so an accurate weight can be determined. In case you do become uncomfortable during the densitometry testing, 3 researchers will be present at all times to ensure your safety and recovery from the tank. Skinfold measurements will be taken with calipers while girths will be taken using a tape measure to determine your muscle mass. The densitometry and muscle mass testing will take a total of about one hour. Therefore, you will donate a total of 2 hours if you choose to take part in the study.

Please answer the following questions so we can determine if you meet the criteria for the study.

YES	NO	
____	_____	1. Have you ever had a metallic foreign body in your eye?
		Do you have:
____	____	cardiac pacemaker, wires or defibrillator?
____	____	artificial cardiac valve? If YES, what make and model?_____
____	____	aneurysm clip?
____	____	ear implant?
____	____	eye implant?
____	____	electrical stimulator for nerves and bones?
____	____	other implanted device(s) or Metallic objects in your body?

Explain _____

____	_____	Have you ever had surgery in your upper arm, forearm, thigh, or calf?
____	_____	Are you claustrophobic?
____	_____	Do you weigh over 260 lbs. (120 kg)? If YES, how much?_____

Because MRI involves a magnetic field, you will not be permitted to take part in the study if you have answered "YES" to any of the above questions. If you have claustrophobia, hydrophobia (fear of water) or cannot climb a ladder, you will not be allowed to participate in the study because of the densitometry. If any of these conditions apply to you, or you have answered "YES" to any of the above questions, please notify the researcher.

All information obtained as part of this research project will be held in the strictest of confidence and will be available to Richard Schaan and Drs. Preston Wiley, Carla Wallace and Michael Hawes and the thesis committee.

It is anticipated that a scientific paper and a Masters thesis will be published based on the information gained in this study. At no time will you be mentioned by name or in such a way that you could be identified personally. The MRI and densitometry data will be secured in a password-protected account and file during the study to ensure your confidentiality, with original MRI files remaining at the MRI Center at Foothills Hospital until they are purged after six months. Once the study is complete, the files will be backed-up and stored for the standard five years in a locked filing cabinet which is only accessible by myself (Richard Schaan). The original MRI and densitometry data will be erased to ensure confidentiality.

Your signature on this form indicates that you have understood to your satisfaction the information regarding participation in the research project and agree to participate as a subject. In no way does this waive your legal rights nor release the investigators, sponsors, or involved institutions from legal and professional responsibilities. You are free to withdraw from the study at any time without jeopardizing your health care. Your continued participation should be as informed as your initial consent, so you should feel free to ask for clarification or new information throughout your participation. If you have further questions concerning matters related to this research, please contact:

Richard Schaan 220-8986

If you have any questions concerning your rights as a possible participant in this research, please contact the Office of Medical Bioethics, Faculty of Medicine, University of Calgary, at 220-7990.

_____	_____
Participant's Signature	Date
_____	_____
Investigator and/or Delegator's Signature	Date
_____	_____
Witness' Signature	Date

A copy of this consent form has been given to you to keep for your records and reference.

Appendix D

Anthropometric Descriptions

The anthropometric variables that were measured are very specific sites that are defined as follows:

Stature (height) - All stature measurements should be taken with the subject barefoot. The Frankfort plane refers to the position of the head when the line joining the orbitale (lower margin of eye socket) to the tragion (notch above tragus of the ear) is horizontal.

Stature against wall:

- Subject stands erect, feet together against a wall on a flat surface at a right angle to the wall mounted stadiometer.
- Stadiometer consists of a vertical board with an attached metric rule and a horizontal headboard that slides to contact the vertex.
- The heels, buttocks, upper back and (if possible) cranium should touch the wall.
- Subjects head should be in the Frankfort plane, arms relaxed at sides.
- Subject is instructed to inhale and stretch up.

- Measurer slides the headboard of the stadiometer down to the vertex and records the measurement to the nearest 0.1 cm.

Girths

Maximum Upper Arm Girth (cm)

- The girth measurement of the upper arm at the insertion of the deltoid.
- Subject stands erect with the arm abducted to the horizontal, measurer stands behind the arm of the subjects, marks the insertion of the deltoid and measures the girth perpendicular to the long axis of the arm.

Maximum Forearm Girth (cm)

- The maximum circumference at the proximal part of the forearm (usually within 5 cm of the elbow).
- Subject stands erect with the arm extended in the horizontal plane; measurer stands behind the subject's arm and moves the tape up and down the forearm (perpendicular to the long axis) until the maximum circumference of the forearm is located.

Mid Thigh Girth (cm)

- The girth taken at the midpoint between the greater trochanter and the head of the fibula.
- Subject stands erect, feet 10 cm apart and weight evenly distributed; measurer crouches to the right side, palpates and marks the trochanterion and the tibiale laterale. The midpoint is found using a tape or anthropometer.
- The girth is taken at this level, perpendicular to the long axis of the thigh.

Maximum Calf Girth (cm)

- Subject stands erect, feet 10 cm apart and weight evenly distributed; measurer crouches to the right side and moves the tape up and down the calf, perpendicular to the long axis until the greatest circumference is located.

Skinfolds

Upper Arm Skinfold (Triceps)

- Vertical skinfold raised on the posterior aspect of the medial triceps, exactly halfway between the olecranon process and the acromion process when the hand is supinated.

Forearm Skinfold (lateral)

- A vertical skinfold taken at the level of maximum forearm girth on the lateral aspect of the forearm with the hand supinated.

Mid Thigh Skinfold

- Vertical skinfold raised on the anterior aspect of the thigh midway between the inguinal crease and the proximal border of the patella.

Medial Calf Skinfold

- A vertical skinfold taken on the medial aspect of the calf at the level of maximum calf girth; subject stands with the right foot on a platform, flexing the knee and hip to 90°.

Appendix E

Computer Prompts - Data Analysis

The following are the protocols and commands used to analyze the MRI files. Analysis was performed on a Sun Computer System unless otherwise noted, after the raw MRI files were transferred via FTP.

1. A raw MRI file contains data from several slices, with each slice containing "water+fat" and "water-fat" data. These slices must first be separated so further analysis can be performed. This was done using the in-house program "rawmssplit" (Crawley, 1997). The following command style was used:

> rawmssplit pixels #slices prefix1 prefix2 < P02056

e.g. > rawmssplit 256 3 r1 r2 < P02056

This produced six files: r1.sl0 r2.sl0

r1.sl1 r2.sl1

r1.sl2 r2.sl2

r1.xxx and r2.xxx files correspond to the "w-f" and "w+f" files respectively.

2. The in-house program "rawnhtofold" was then executed to change the files from signa to float data.

e.g. > rawnhtofold 256 < r1.sl0 > r11.sl0

3. Once converted to float data, the in-house program "phasefit" was then used to correct for field inhomogeneities and convert the data so it was IFFT'd.

e.g. > phasefit r11.sl0 and input the following protocol on request:

Negative Frequency: 32

Phase Estimation Technique: 1

Model Order: 2

Inversion Recovery Image: Yes

Convergence Tolerance: .1

Wrap Phase: No

Save Phase Image: No

Save Phase Corrected Image: Yes

The image can now be reconstructed using the program "Viewdiff" (Chow & Crawley, 1996).

To access "Viewdiff", "Open Windows" must be activated on the Sun system, using the command: > ow

With "Open Windows" active, the following command was input into the command tool:

> viewdiff

When "Viewdiff" was open, the phase correction was checked by selecting the options to reconstruct the image as an IFFT imaginary image.

The reconstructed image would appear black with a white spot in the middle, indicating good phase correction.

Once the phase correction was determined, the image was reconstructed by selecting the option for a magnitude float image. With the image present, the Colormap was selected from the "Tools" menu. The brightness and contrast were then set to the following parameters:

Brightness: 90

Contrast: 108

Start: 1 Stop: 217 Center: 80

Using the "zoom" module, the image was enlarged using the bicubic function 2x.

The image was then saved using the Snapshot tool, which is part of the Unix Open Windows Command. A snapshot was taken and saved as a Sun Raster image.

All the images were then transferred to an Apple Power Macintosh using the program "Fetch 3.0.1".

Once on the Macintosh, all Sun Raster images were converted to TIFFs by selecting the "batch conversion" option in the program "Graphic Converter".

In TIFF format, the images were opened in Adobe Photoshop. The following commands were performed in Photoshop:

The lasso tool was selected; the interstitial region plus some residual subcutaneous was selected. Once selected the region was "copied".

A new file was opened and the image was "pasted".

The new image was altered using the "eraser" and "magic wand" tools to remove any subcutaneous adipose and the bone.

In the "Image" menu, "Adjust" was selected and then "threshold":

> Image > Adjust > Threshold

In the "Threshold", 195 was input. This created a black & white image, with all pixels having an intensity above 195 white, and lower intensities were turned black.

In the "Image" menu, "histogram was selected:

> Image > Histogram

The output of the histogram is the total number of pixels in the image, and the number of pixels that are white. Therefore, a percentage by area could be calculated, and subsequent conversions could be made.

Appendix F

Equations for Densitometry, Residual Volume & Muscle Mass

I. Anthropometric Muscle Mass Equations (Martin *et. al.* 1990):

Corrected Thigh Girth (CTG) (cm) = thigh girth (cm) - π (front thigh skinfold (mm) /10)

Corrected Calf Girth (CCG) (cm) = calf girth (cm) – π (medial calf skinfold (mm) /10)

FG = Forearm Girth (cm)

All measurements are in centimeters.

kg Skeletal Muscle = [ht * (0.0553 CTG^2 + 0.0987 FG^2 + 0.0331 CCG^2) – 2445] * 0.001

II. Densitometry & Residual Volume Equations:

a) Residual Volume (RV) (in litres) Wilmore *et. al.* 1980:

$$RV = \frac{[VO_2 * FeN_2 - DS]}{0.798 - FeN_2} * BTPS$$

where:

VO_2 = the initial volume of oxygen used in the bag (L)

FeN_2 = the fraction of nitrogen after the testing; expressed as a decimal percentage. $FeN_2 = [100\% - (\%O_2 + \%CO_2)] / 100$

DS = dead space in the mouthpiece and breathing apparatus (L).

BTPS = body temperature pressure saturation correction factor which corrects the volume of measured gas to ambient conditions of the lung.

b) Body Density Equations:

$$\text{Body Density (kg/L)} = \frac{\text{weight in air (kilograms)}}{\frac{(\text{wt in air} - \text{wt. In water} - \text{tare wt.})}{\text{water temp. correction}} - \text{trapped air}}$$

where:

trapped air (L) = RV (L) + tubing dead space (L) + 0.1 L; the conventional allowance for gastro-intestinal gases).

All weights for the previous calculation are in kilograms.

% Fat (Siri, 1956): $\%\ \text{Fat} = [(4.95 / \text{body density}) - 4.50] * 100$

Appendix G

MRI Calculations

MRI Conversion Equations:

a) The initial values obtained from the MRI analysis are in terms of percent adipose (by area). This is from taking the number of adipose pixels and dividing by the total number of pixels in the interstitial area. Unfortunately, this value is limited because it has no common units to compare values. Therefore, the pixel values must be converted. So the MRI values can be compared with total body lipid values, the end value must be in terms of mass.

Adipose area is converted to a volume by multiplying the pixel area by the scan thickness. This should not introduce any errors. A pixel is visualized as a two dimensional area when in fact the intensity associated with it is averaged from the depth that it is taken from.

e.g. # adipose pixels x 0.0175 cm^3 = adipose tissue volume (cm^3)

0.0175 is the volume of a voxel. (Field of View is 24 cm^2 with a 256 x 256 matrix in the field. Therefore, pixel area is 0.09375 x 0.09375 = 0.00879 cm^2 with a depth of 2.0 cm, yielding the volume of 0.0175 cm^3/pixel.)

This volume can be converted to an adipose tissue mass by assuming a constant density. Adipose tissue density according to the literature (Thomas, 1962) is 0.9196 g/ml. This produces an adipose tissue mass.

e.g. 50 cm^3 x 0.9196 g/ml = 45.98 g of adipose tissue.

Because densitometry quantifies lipid, not adipose, the adipose tissue mass must be converted to a lipid mass. This was accomplished by assuming a constant fraction of adipose tissue is lipid. From Thomas (1962), the assumed constant is 0.85. (85% of adipose is lipid.) This yielded a mass of lipid which was compared with total body fat.

b) Because most references to interstitial lipid are in comparison to skeletal muscle mass, the muscle tissue within the scanned area was converted to a mass using similar procedures to those above.

Volume was converted using the same formula.

Mass of the muscle tissue was determined by assuming a constant fat-free density of 1.07 g/ml (Allen *et. al.* 1959).

Because the same assumptions and calculations were performed on both the muscle and interstitial lipid pixels, any systematic errors should be eliminated.

Appendix H

Anthropometric Screening Data

The following table indicates the initial screening value for total body fat from each subject according to the technique of Parizkova (1978) and the value later determined by densitometry.

Table H1: Total body data from initial anthropometric screening (Parizkova, 1978) and densitometry.

Subject:	Total Body Fat (%)	
	Parizkova (1978)	Densitometry
1	27.6	36.86
2	13.2	12.60
3	13.8	12.60
4	7.5	8.76
5	12.9	10.51
6	13.2	9.61
7	12.4	14.79
8	29.7	33.87
9	16.2	13.05
10	13.5	13.96
11	12.9	13.65
12	12.1	11.96
13	17.1	20.08
14	21.0	19.37
15	14.1	12.96
16	9.5	5.26
17	8.2	7.95
18	34.4	31.98
19	16.33	15.53
20	19.36	25.41

Appendix I

MRI Interstitial Lipid Slice Data

Table I1: Percent interstitial lipid for each slice from all subjects. Slices are listed from most proximal to most distal from the respective limb segment.

Subject	Forearm	Upper Arm	Upper Leg	Lower Leg
1	13.98	4.16	9.05	9.30
	6.21	3.86	9.26	17.27
	6.95	3.20	8.82	12.23
2	15.89	1.94	4.50	3.14
	4.47	6.64	4.19	3.98
	8.36	2.34	4.85	1.97
3	14.31	3.44	5.58	3.29
	3.66	1.90	5.84	2.93
	3.47	3.37	5.36	2.14
4	6.25	2.74	4.08	1.61
	4.30	3.48	3.89	1.93
	4.19	2.13	4.31	1.73
5	7.35	3.13	3.61	3.23
	4.00	3.65	3.39	3.66
	2.53	2.99	3.87	3.04
6	6.87	2.60	3.25	2.54
	3.51	2.97	3.73	3.54
	2.08	2.36	2.73	2.62
7	12.76	3.56	5.08	2.41
	1.29	3.63	5.67	2.70
	2.16	2.92	4.43	2.03
8	13.06	1.82	7.02	5.30
	5.83	6.29	7.80	17.43
	11.17	3.82	6.20	6.07
9	10.76	2.39	5.13	5.92
	2.44	4.30	5.76	5.42
	7.05	1.41	4.44	5.04
10	9.74	6.02	5.60	2.60
	3.63	3.95	6.30	5.47
	4.59	4.16	4.86	2.04
11	6.18	6.17	4.10	3.39
	2.12	2.70	4.92	7.79
	2.59	7.08	3.32	4.77

12	9.53	3.27	4.25	2.94
	2.31	3.13	4.80	2.26
	5.58	3.89	3.70	1.98
13	5.68	5.50	4.63	3.00
	2.26	5.84	4.25	3.41
	4.07	3.49	5.05	3.12
14	7.77	4.36	4.33	1.73
	2.43	4.24	4.46	7.14
	3.85	3.65	4.20	3.62
15	7.12	2.32	3.75	2.24
	2.81	4.82	4.02	3.49
	4.04	2.78	3.54	4.45
16	6.81	2.03	1.63	0.96
	2.13	1.73	1.67	0.74
	3.93	1.64	1.73	0.50
17	4.35	5.12	1.51	1.58
	4.18	2.29	1.59	3.38
	4.09	3.84	1.41	2.88
18	11.27	6.01	3.40	5.69
	5.19	3.12	2.92	11.65
	4.98	2.47	3.90	8.03
19	10.90	4.17	1.75	2.57
	5.03	4.16	1.54	3.69
	4.43	5.12	1.92	2.74
20	13.54	2.90	3.93	1.21
	4.51	4.66	4.16	4.82
	5.66	3.15	3.72	1.90

Appendix I

Interstitial Limb Segment Histograms

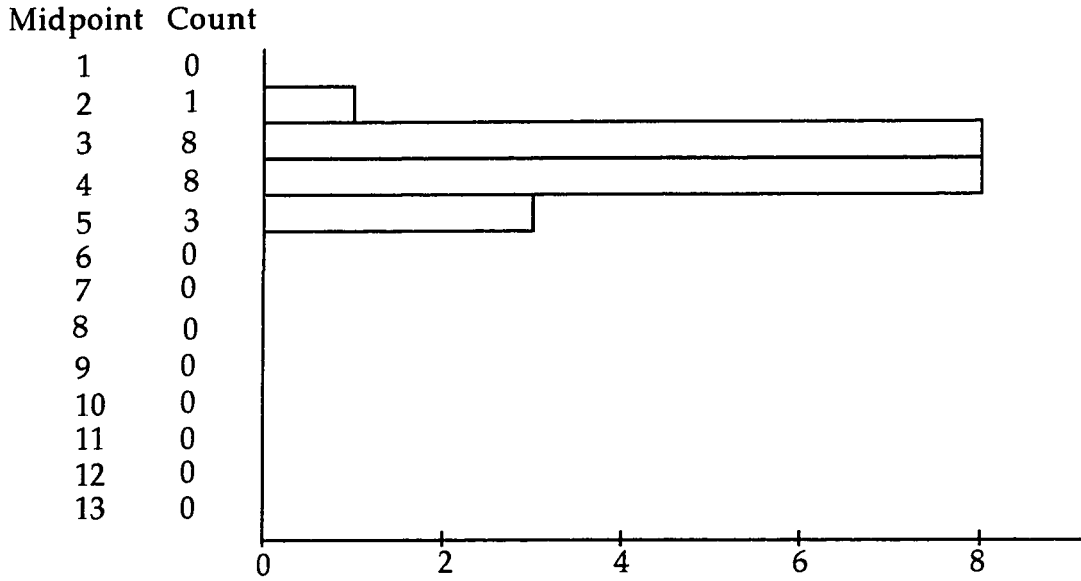

Figure J.1: Histogram of the percent interstitial lipid data for the upper arm, indicating the distribution of the upper arm slices.

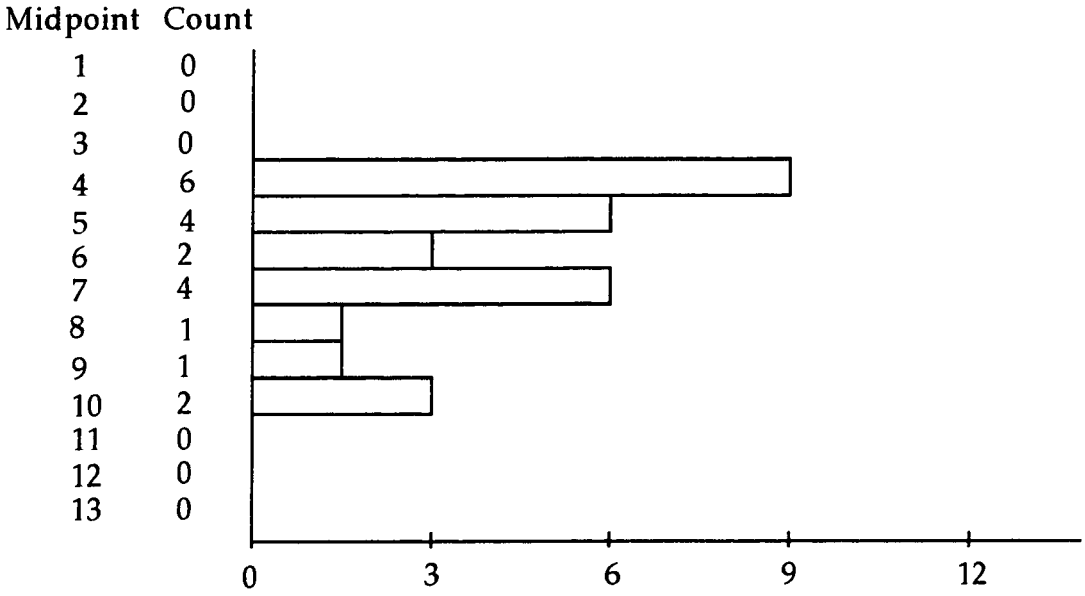

Figure J.2: Histogram of the percent interstitial lipid data for the forearm, indicating the distribution of the forearm slices.

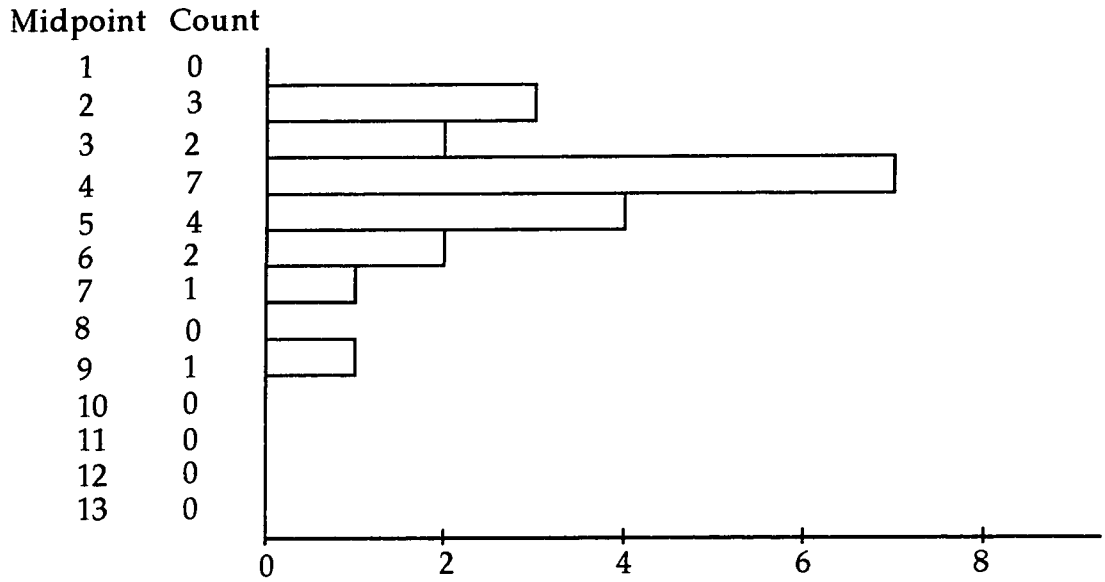

Figure J.3: Histogram of the percent interstitial lipid data for the upper leg, indicating the distribution of the upper leg slices.

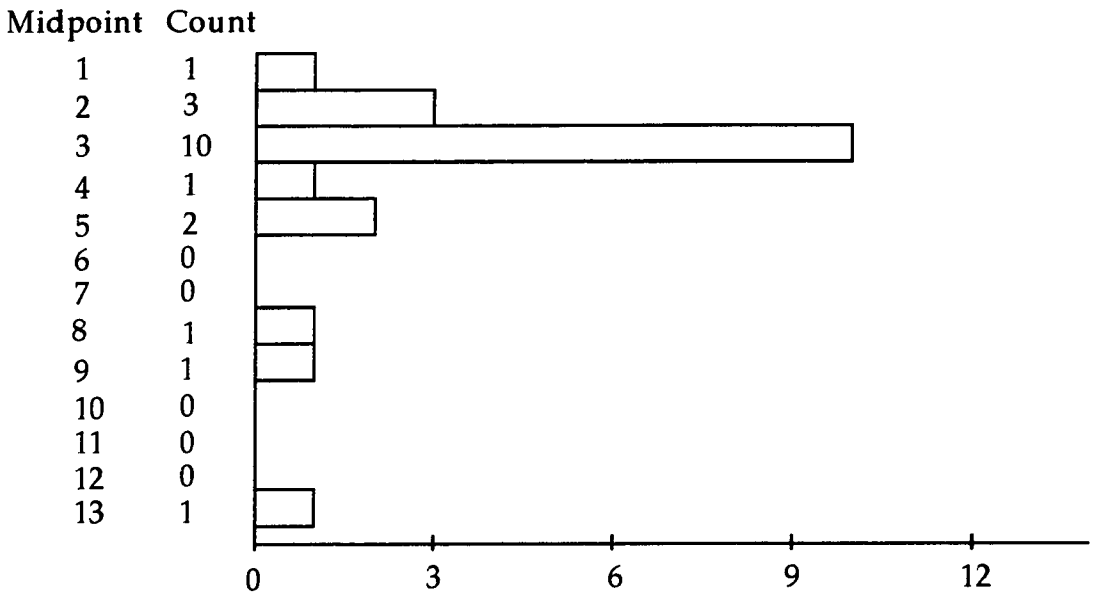

Figure J.4: Histogram of the percent interstitial lipid data for the lower leg, indicating the distribution of the lower leg slices.